Mechanism of 2-Chloro-(ε-amino-Lys$_{75}$)-[6-[4-(*N*,*N*-diethylamino)phenyl]-1,3,5-triazin-4-yl]calmodulin Interactions with Smooth Muscle Myosin Light Chain Kinase and Derived Peptides†

Katalin Török‡ and David R. Trentham*

National Institute for Medical Research, Mill Hill, London NW7 1AA, United Kingdom

Received June 20, 1994; Revised Manuscript Received August 12, 1994®

ABSTRACT: The mechanism of the interactions of 2-chloro-(ε-amino-Lys$_{75}$)-[6-[4-(*N*,*N*-diethylamino)phenyl]-1,3,5-triazin-4-yl]calmodulin (TA-calmodulin) with smooth muscle myosin light-chain kinase (MLCK) and two 17-residue peptides, Ac-R-R-K-W-Q-K-T-G-H-A-V-R-A-I-G-R-L-CONH$_2$ (Trp peptide) and Tyr peptide, in which W is replaced by Y, were studied by measurements of equilibrium and transient fluorescence changes in the nanomolar range. Most reactions were carried out in 100 μM $CaCl_2$ at ionic strength 0.15 M, pH 7.0, and 21 °C. In each case association of MLCK or peptide to TA-calmodulin could be described by a two-step process, a bimolecular step and an isomerization. In the case of the interaction between TA-calmodulin and Tyr peptide it was shown that the isomerization involved the binary complex of TA-calmodulin and Tyr peptide as opposed to an isomerization of either TA-calmodulin or Tyr peptide in isolation. These distinctions depended in part on development for transient kinetic experiments of a general theory to quantify relative phase amplitudes in two-step mechanisms. The kinetics for all three association reactions were then interpreted in terms of a bimolecular association (rate constants k_{+1} and k_{-1}) followed by an isomerization of the binary complex (rate constants k_{+2} and k_{-2}). For the interaction of TA-calmodulin and Tyr peptide, values of the rate constants are k_{+1}, 8.8 × 10^8 M^{-1} s^{-1}; k_{-1}, 5.7 s^{-1}; k_{+2}, 0.38 s^{-1}; and k_{-2}, 0.65 s^{-1}. The fluorescence intensities (λ_{ex} 365 nm, λ_{em} > 400 nm) of TA-calmodulin, the initial binary complex of TA-calmodulin and Tyr peptide, and the isomerized binary complex are in the ratio 1:2.8:1.3. Analogous mechanisms were found for TA-calmodulin binding to Trp peptide and to MLCK, but values for the rate constants and relative fluorescence intensities of the binary complexes were generally not so completely defined. Values for the Trp peptide and MLCK, respectively, are k_{+1}, 8.8 × 10^8 M^{-1} s^{-1} and 1.1 × 10^8 M^{-1} s^{-1}; (k_{+2} + k_{-2}), 0.97 s^{-1} and 1.3 s^{-1}; and $k_{-1}k_{-2}/(k_{+2} + k_{-2})$, 0.0079 s^{-1} and 0.025–0.056 s^{-1}. Equilibrium dissociation constants (K_d) for interactions of TA-calmodulin and targets determined from these data are Tyr peptide, 4.1 nM; Trp peptide, 0.011 nM; and MLCK, 0.23–0.51 nM. K_d values for calmodulin and the ligands were Tyr peptide, 3.6 nM; Trp peptide, 0.006 nM; and MLCK, 0.10–0.22 nM. Possible structural and physiological implications of these data are discussed.

The central role of calmodulin as part of the cell's machinery for transmitting changes of Ca^{2+} concentration so as to regulate cellular function is well established. The structural basis for the interaction of calcium–calmodulin with target peptides has received great impetus from determination of structure to atomic resolution using NMR[1] spectroscopy and X-ray diffraction (Babu et al., 1988; Ikura et al., 1992; Meador et al., 1992, 1993). The thermodynamic and kinetic basis for the functional properties of calmodulin, in particular in its interactions with MLCK, has been investigated using a variety of physical chemistry approaches [e.g., Johnson et al. (1981), Kasturi et al. (1993), Klee (1988), and Milos et al. (1988)]. Nevertheless, the latter approaches have frequently been susceptible to limitations on two counts: First, the sensitivity of probes used to monitor the thermodynamic or structural changes is generally not capable of detecting changes at nanomolar concentrations that may be the appropriate range to study the interactions because of comparable intrinsic dissociation constants. Experiments in the nanomolar concentration range are also frequently necessary to distinguish bimolecular diffusion-controlled association steps from protein isomerizations. Second, homogeneous protein or peptide preparations are generally needed, with respect to both primary amino acid sequence and site of probe labeling, for delineation of kinetic steps in protein–ligand and protein–protein interactions.

Given the new structural information, together with structural variants made available through molecular biological methods, it is important to investigate and/or reinvestigate the mechanisms whereby calmodulin interacts with its target peptides in the presence of calcium. This provides an essential link between atomic resolution structures and cellular function.

For this purpose we have used a highly fluorescent and environmentally sensitive reagent, TA-Cl (Cowley et al., 1991; Shaw & Ward, 1967).[2] TA-Cl labeled calmodulin preferentially at Lys$_{75}$ in the presence of Ca^{2+}, and the specifically labeled TA-calmodulin (**I**, Figure 1) was isolated by HPLC.

† This work was supported by the National Institutes of Health Grant HLB 15835 to the Pennsylvania Muscle Institute and the Medical Research Council, U.K.

* To whom correspondence should be addressed.

‡ Present address: Department of Physiology, University of College London, Gower St., London WC1E 6BT, U.K.

® Abstract published in *Advance ACS Abstracts*, September 15, 1994.

[1] Abbreviations: EGTA, ethylene glycol bis(β-aminoethyl ether)-*N*,*N*,*N*′,*N*′-tetraacetic acid; F-moc, 9-fluorenylmethoxycarbonyl; FPLC, fast protein liquid chromatography; HPLC, high-performance liquid chromatography; MES, 2-(*N*-morpholino)ethanesulfonic acid; MLC, myosin regulatory light chains from smooth muscle; MLCK, smooth muscle myosin light-chain kinase; NMR, nuclear magnetic resonance; SDS–PAGE, sodium dodecylsulfonate–polyacrylamide gel electrophoresis; TA-calmodulin, 2-chloro-(ε-amino-Lys$_{75}$)-[6-[4-(*N*,*N*-diethylamino)-phenyl]-1,3,5-triazin-4-yl]calmodulin; TA-Cl, 2,4-dichloro-6-[4-(*N*,*N*-diethylamino)phenyl]-1,3,5-triazine; TFA, trifluoroacetic acid; Tyr peptide, Ac-R-R-K-Y-Q-K-T-G-H-A-V-R-A-I-G-R-L-CONH$_2$; Trp peptide, Ac-R-R-K-W-Q-K-T-G-H-A-V-R-A-I-G-R-L-CONH$_2$.

0006-2960/94/0433-12807$04.50/0

Here we analyze the mechanism whereby TA-calmodulin interacts with MLCK and two 17-residue peptides (Trp peptide and Tyr peptide) that correspond to the sequence in the calmodulin target area of MLCK except that Tyr replaces Trp in the Tyr peptide. The complexity and detail of the results is such that reported experiments are restricted to being done in the presence of Ca^{2+}.

The results are informative in several respects. First, kinetically determined dissociation constants of TA-calmodulin and Tyr peptide can be directly compared with those obtained from equilibrium measurements. Second, the time courses and amplitudes of the fluorescence changes indicate two-step binding of TA-calmodulin to the Tyr peptide in which reactants associate in a diffusion-controlled manner. Third, the predominant mechanism can be described as one in which protein–peptide isomerization occurs after peptide binding rather than being a protein or peptide isomerization before the binding step. Fourth, the Trp peptide and MLCK also bind in a two-step mechanism to TA-calmodulin. Finally, competition experiments between TA-calmodulin and calmodulin for MLCK and its derived peptides show that in each case calmodulin binds 1–3-fold more tightly than TA-calmodulin.

MATERIALS AND METHODS

Proteins and Peptides: Preparation and Characterization. Calmodulin was purified from pig brain as described by Török et al. (1992) for bovine brain. The molecular mass determined from its electrospray mass spectrum was 16 790.9 Da and equals that of bovine brain calmodulin (16 790.3) (Watterson et al., 1980). This indicates that the amino acid sequences and posttranslational modifications of pig and bovine brain calmodulins are identical. MLCK was copurified with caldesmon from bovine rumen (Walsh et al., 1982) by an extension of the procedure described by Ikebe et al. (1987) for turkey gizzard MLCK. MLCK was separated from caldesmon by two cycles of phosphocellulose chromatography. It was rapidly frozen and stored in aliquots at −80 °C. MLC were purified from the myofibrillar pellet of rumen remaining after the extraction of MLCK and caldesmon. MLC were isolated essentially as described by Hathaway and Haeberle (1983), stored as a lyophilized powder, and characterized by SDS–PAGE.

TA-Calmodulin was prepared by labeling pig brain calmodulin with TA-Cl in the presence of Ca^{2+}, based on previous experience of selective reactivity of Lys_{75} toward electrophilic reagents (Giedroc et al., 1985, 1987; Mann & Vanaman, 1987, 1988; Newton & Klee, 1989). Calmodulin (15 mg, 1 mg/mL) was treated with 200 μM TA-Cl (Cowley et al., 1991) (from 2.5 mM TA-Cl in dimethylformamide) in 20 mM $CaCl_2$ and 100 mM Tris adjusted to pH 8.5 with HCl. The solution was incubated at 22 °C in the dark and stirred occasionally. The progress of the reaction was monitored spectrophotometrically by the slow change in absorption maximum from 403 to 365 nm (Cowley et al., 1991; Cowley & Pasha, 1981; Shaw & Ward, 1967). The reaction was terminated by gel filtration on Bio-Gel P4 equilibrated in H_2O to remove both insoluble and soluble excess reagent. The Bio-Gel P4 gel-filtered reaction mixture of TA-calmodulin was purified by FPLC (Mono Q HR 10/10 column) and HPLC (Vydac 218 TP54 reverse-phase C_{18} column) to homogeneity [monitoring absorption at 215 nm and fluorescence at 360 (excitation) and 455 nm (emission)] using protocols similar to those described by Mann and Vanaman (1988).

Tyr peptide and Trp peptide were synthesized by F-moc technology and purified to homogeneity by reverse-phase HPLC with a gradient (0.5% change/min) of 0.1% TFA in H_2O to 0.082% TFA in CH_3CN on a Waters Deltapak C_{18} column (30 mm × 30 cm) at a flow rate of 2.0 mL/min. Protonated masses of 2053 and 2076 Da determined by fast atom bombardment mass spectrometry confirmed the structures of the Tyr and Trp peptides, respectively.

TA-Calmodulin has an ϵ_0 value of 40 100 M^{-1} cm^{-1} at a λ_{max} of 377 nm measured in a solution of 1 mM EGTA, 100 mM KCl, 2 mM $MgCl_2$, and 50 mM K-MES at pH 7.0 and 21 °C. Its mass determined from its electrospray mass spectrum was 17 052.4 (theory 17 052.1, based on 16 791.4 for calmodulin). Amino acid analytic methods of tryptic peptide analysis, amino acid sequencing, and fast atom bombardment mass spectrometry of peptide showed that 99% of the labeling was at Lys_{75}. TA-calmodulin was an activator of adenosine 3′,5′-cyclic monophosphate phosphodiesterase from beef heart (Boehringer Mannheim) with a K_m of 0.45 nM and the same V_{max} as calmodulin (K_m 0.13 nM). TA-Calmodulin was an inhibitor of MLCK with K_i 12.6 nM (calmodulin K_m 3.5 nM). These steady-state studies also showed that calmodulin was present at <1% in TA-calmodulin. The fluorescence of TA-calmodulin increased 5.5-fold upon Ca^{2+} binding and was accompanied by a small hypsochromic shift in excitation (380 to 365 nm) and emission (420 to 410 nm) maxima. In titrations of Ca^{2+} into TA-calmodulin, the fluorescence increase was saturated by 4 μM free Ca^{2+} measured in a solution of 1 mM EGTA, 100 mM KCl, 2 mM $MgCl_2$, and 50 mM K-MES at pH 7.0 and 21 °C.

Other protein and peptide concentrations were determined spectroscopically using the following molar extinction coefficients (ϵ_0): calmodulin, ϵ_0 = 3300 M^{-1} cm^{-1} at 275 nm in the absence of Ca^{2+} (Klee, 1977); Tyr peptide, ϵ_0 = 1400 M^{-1} cm^{-1} at 275 nm, and Trp peptide, ϵ_0 = 5700 M^{-1} cm^{-1} at 278 nm, both in aqueous solution at pH 7.

Equilibrium and Transient Kinetic Experiments. Equilibrium binding experiments were carried out on a SLM Instruments Inc. photon-counting fluorometer. Stopped-flow experiments were carried out in HI-TECH PQ/SF-51MX and HI-TECH SF-61MX multimixing stopped-flow spectrofluorometers each equipped with a Hg lamp, a monochromator, photomultiplier, and amplifier unit. Exciting light was passed through the monochromator (365 nm for TA excitation, 290 nm for Trp excitation) and emitted light was passed through a cutoff filter (>400 nm) for TA fluorescence and a 350-nm interference filter for Trp fluorescence. TA-Calmodulin was reasonably resistant to photobleaching. In stopped-flow experiments the photobleaching rate was 0.1% of the fluorescence s^{-1}.

[2] The preparation, purification, characterization, and enzymatic properties of TA-calmodulin were carried out in collaboration with D. J. Cowley, B. D. Brandmeier, S. Howell, and A. Aitken. Further details of TA-calmodulin are available on request. TA-Cl contained 8.1% 2,4-dichloro-6-(*N*-ethylanilino)-1,3,5-triazine. This reagent also labeled calmodulin at Lys_{75} but did not absorb near-UV light above 330 nm or fluoresce on near-UV irradiation (Shaw & Ward, 1967). TA-Calmodulin contained 8.6% Lys_{75} modified with this reagent as determined by electrospray mass spectra. The contaminant calmodulin appeared to interact with MLCK and adenosine 3′,5′-cyclic monophosphate phosphodiesterase identically with TA-calmodulin but did not exhibit any fluorescence in the region studied. All concentrations of TA-calmodulin are corrected for its presence. Subsequent to the main body of research reported here, TA-Cl was synthesized free of 2,4-dichloro-6-(*N*-ethylanilino)-1,3,5-triazine (Golesworthy et al., 1962). TA-Calmodulin prepared from this reagent had identical properties to that of TA-calmodulin corrected for contaminant calmodulin as described above.

Data were collected via an analog-to-digital converter board by an IBM PC. Exponential functions of the form $\Lambda \exp(-\lambda t)$ or $[\Lambda_1 \exp(-\lambda_1 t) + \Lambda_2 \exp(-\lambda_2 t)]$ were fitted to the data by a nonlinear least-squares algorithm based on the Marquardt method and standard errors of the estimate (Bevington, 1969) are quoted (Figures 3A and 5A). For graphical analysis of data points, linear (Figures 2C, 4C, and 6B) or nonlinear (Figures 1 and 5B) least-squares fits are made and standard errors are quoted. Where data do not warrant this treatment, the limits within which the measured value is expected to lie are stated. Simulations of reaction schemes were done using a software package KSIM provided by N. C. Millar.

All experiments except those specified otherwise were carried out at 21 °C in a solution containing 100 mM KCl, 100 μM $CaCl_2$, 2 mM $MgCl_2$, and 50 mM MES adjusted to pH 7.0 with KOH.

DESIGN AND THEORY OF KINETIC EXPERIMENTS

In this section we summarize the experimental design and theoretical analysis necessary for interpretation of the kinetic experiments. The theory is based on classical analysis in the transient kinetic field (Fersht, 1984; Frost & Pearson, 1961; Gutfreund, 1972). One parameter that is important to our experiments is the relative amplitude of phases observed in biphasic transients. We describe the general theory in a manner that allows this measured parameter, here relative fluorescence intensity, to be easily related to mechanisms being tested and distinguished from one another. We begin by focusing on analysis specific to our experiments.

Design and Theory of Specific Experiments. As will be seen, the data indicate that when TA-calmodulin interacts with a peptide target or MLCK, at least two kinetically resolvable processes occur, one second-order in reactants and one first-order. These are most readily interpreted in terms of an association step followed by an isomerization (Scheme 1). In Scheme 1, P refers to Tyr peptide, Trp peptide, or MLCK, TA-cal is unliganded TA-calmodulin, and TA-cal·P and TA-cal·P* are protein–peptide or protein–MLCK complexes of TA-cal and P. The fluorescence intensities of TA-cal, TA-cal·P, and TA-cal·P* are defined as F_1, F_2, and F_3. In the experimental records fluorescence is frequently normalized against that of TA-cal (i.e., $F_1 = 1$).

Scheme 1

$$\underset{(F_1)}{\text{TA-cal}} + \text{P} \overset{k_{+1}}{\underset{k_{-1}}{\rightleftharpoons}} \underset{(F_2)}{\text{TA-cal·P}} \overset{k_{+2}}{\underset{k_{-2}}{\rightleftharpoons}} \underset{(F_3)}{\text{TA-cal·P*}}$$

Under conditions where the bimolecular step is much faster than the isomerization and in which [P] $\gg$ [TA-calmodulin] and k_{+1}[P] $\gg k_{-1}$, the initial fluorescence intensity change corresponding to $(F_2 - F_1)$ occurs in an exponential process at a rate k_{obs} given by

$$k_{obs} = k_{+1}[\text{P}] + \text{constant} \tag{1}$$

where the constant either equals k_{-1} or is a function of k_{+2}, k_{-1}, and k_{-2}. The isomerization follows the bimolecular step and is accompanied by a fluorescence change occurring as an exponential process at a rate k^*_{obs} given by

$$k^*_{obs} = k_{+2} + k_{-2} \tag{2}$$

where the final fluorescence amplitude, F_∞, is given by

$$F_\infty = (k_{+2}F_3 + k_{-2}F_2)/(k_{+2} + k_{-2}) \tag{3}$$

Scheme 2

$$\text{TA-cal·P*} \overset{k_{-2}}{\underset{k_{+2}}{\rightleftharpoons}} \text{TA-cal·P} \xrightarrow{k_{-1}} \text{TA-cal} + \text{P}$$

P trapped by calmodulin

The dissociation rate of P from TA-calmodulin may be measured by mixing a solution of TA-calmodulin and several-fold molar excess of P with a large molar excess of calmodulin as in Scheme 2. The fluorescence intensity, F_t, will change as a function of time in either a monophasic or biphasic process. The monophasic response occurs if the equilibrium between TA-cal·P and TA-cal·P* strongly favors TA-cal·P* (i.e., $k_{+2} \gg k_{-2}$) when the observed rate constant, k_{diss}, is given by

$$k_{diss} = k_{-1}k_{-2}/k_{+2} \tag{4}$$

and

$$F_t = F_1 + (F_3 - F_1)\exp(-k_{-1}k_{-2}t/k_{+2}) \tag{5}$$

A monophasic response also occurs if $(k_{+2} + k_{-2}) \gg k_{-1}$, in which case

$$k_{diss} = k_{-1}k_{-2}/(k_{+2} + k_{-2}) \tag{6}$$

and

$$F_t = F_1 - [F_1 - (k_{+2}F_3 + k_{-2}F_2)/(k_{+2} + k_{-2})] \times \exp[-k_{-1}k_{-2}t/(k_{+2} + k_{-2})] \tag{7}$$

Equations 4 and 5 hold if $k_{+2} \gg k_{-1}$ and k_{-2}.

More generally (see below eq 12 and accompanying text), the fluorescence intensity, F_t, will change as a function of time in a biphasic process of the form

$$F_t = F_1 - \Lambda_1 \exp(-\lambda_1 t) - \Lambda_2 \exp(-\lambda_2 t) \tag{8}$$

where, from eq 11, λ_1 and λ_2 are roots of the equation

$$\lambda^2 - (k_{-1} + k_{+2} + k_{-2})\lambda + k_{-1}k_{-2} = 0 \tag{9}$$

The analysis below also shows that the relative fluorescence of the two phases, $\Lambda_1/\Lambda_2 (= F_r$, see eq 14), is given by

$$\frac{\Lambda_1}{\Lambda_2} = -\frac{[k_{-1}k_{-2} - \lambda_2(k_{+2} + k_{-2})]F_1 + (\lambda_2 k_{-2} - k_{-1}k_{-2})F_2 + \lambda_2 k_{+2}F_3}{[k_{-1}k_{-2} - \lambda_1(k_{+2} + k_{-2})]F_1 + (\lambda_1 k_{-2} - k_{-1}k_{-2})F_2 + \lambda_1 k_{+2}F_3} \tag{10}$$

In the case of the interaction of TA-calmodulin and Tyr peptide, analysis of the fluorescence intensities and kinetics allows one to assess whether Schemes 1 and 2 are a necessary and sufficient description of the interaction and whether alternative schemes can be eliminated, such as isomerization of TA-calmodulin or Tyr peptide prior to the association step. The time courses of the fluorescent intensity changes of alternative schemes are described in the Discussion.

Further mechanistic information can be obtained in double-mixing stopped-flow experiments that permit more direct observation of the kinetic properties of the intermediate TA-cal·P. For example, if TA-cal is mixed with P, and then, prior to the isomerization, a second mixing is made with excess calmodulin now acting as a trapping agent for P, it is possible to test at one extreme whether TA-cal·P will decay immediately to TA-cal or whether at the other extreme, TA-cal·P will

Scheme 3

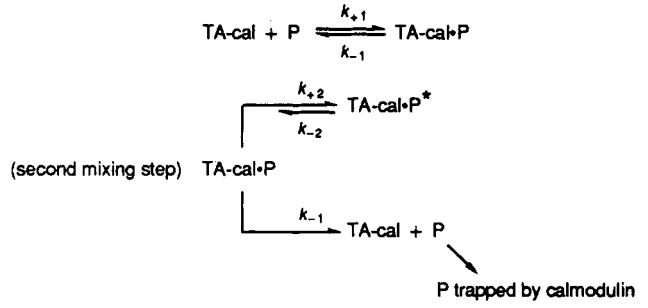

equilibrate to form TA-cal·P* prior to eventual sequestration of P by calmodulin [i.e., there is competition between two pathways determined by the relative values of k_{-1} and $(k_{+2} + k_{-2})$]. The experimental design is illustrated by Scheme 3.

Taken together, Schemes 1–3 provide evaluation of k_{+1} and F_2, partial (possibly complete) evaluation of k_{-1}, k_{+2}, k_{-2}, and F_3, and tests of whether the above schemes are adequate descriptions of the data. Conditions when the analysis may only be partial are when $k_{+2} \gg k_{-2}$ or when $k_{+2} \approx k_{-2} \gg k_{-1}$. In addition, binding of a second peptide to TA-calmodulin, as occurs with Trp peptide, complicates the data analysis.

Displacement experiments such as described by Scheme 2 have a limitation if the observed dissociation rate is slow ($t_{1/2} > 10$ s) because the data are subject to error induced by photobleaching and instrument drift. These problems were reduced by judicious use of shutters and control experiments. Nevertheless, end points and fluorescence time courses beyond 50% of reaction proved to be unreliable. A double-mixing protocol that took advantage of the readily observed TA-cal·P to TA-cal·P* isomerization was devised and is described in Figure 5B and the associated text.

General Theory on Relative Amplitudes in Two-Step Mechanisms. For the purpose of the experiments described here, a generalized two-step mechanism as in Scheme 4 is applicable. An analytical overview of Scheme 4 has been described (Lowry & John, 1910; Frost & Pearson, 1961). The experiments yield fluorescence signals. By solving the differential equations implicit in Scheme 4, the observed fluorescence, F_t, can be related as a function of time to the rate constants and F_a, F_b, and F_c (the fluorescence intensities of A, B, and C respectively).

Scheme 4

$$A \underset{\kappa_{-1}}{\overset{\kappa_{+1}}{\rightleftharpoons}} B \underset{\kappa_{-2}}{\overset{\kappa_{+2}}{\rightleftharpoons}} C$$

To simplify analyses in second-order reaction steps, one of the reactants is presumed to be invariant in concentration. For example, in Scheme 1, if [P] $\gg$ [TA-cal], then $\kappa_{+1} = k_{+1}$[P]. A, B, and C are concentrations of A, B, and C respectively. A_0, B_0, and C_0 and A_∞, B_∞, and C_∞ are concentrations at zero and infinite time. $A' = dA/dt$ with value A'_0 at zero time. B', B'_0, C', and C'_0 are similarly defined. General expressions for A and A' as functions of time are given by $A = A_\infty - \alpha_1 \exp(-\lambda_1 t) - \alpha_2 \exp(-\lambda_2 t)$ and $A' = \alpha_1\lambda_1 \exp(-\lambda_1 t) + \alpha_2\lambda_2 \exp(-\lambda_2 t)$, where λ_1 and λ_2 are roots of the equation

$$\lambda^2 - (\kappa_{+1} + \kappa_{-1} + \kappa_{+2} + \kappa_{-2})\lambda + (\kappa_{+1}\kappa_{+2} + \kappa_{+1}\kappa_{-2} + \kappa_{-1}\kappa_{-2}) = 0 \quad (11)$$

$(\alpha_1 + \alpha_2) = (A_\infty - A_0)$ and $(\alpha_1\lambda_1 + \alpha_2\lambda_2) = A'_0$, from which $\alpha_1 = [A'_0 - \lambda_2(A_\infty - A_0)]/(\lambda_1 - \lambda_2)$ and $\alpha_2 = [A'_0 - \lambda_1(A_\infty - A_0)]/(\lambda_2 - \lambda_1)$. Similar analysis of B and C leads to $B = B_\infty - \beta_1 \exp(-\lambda_1 t) - \beta_2 \exp(-\lambda_2 t)$ and $C = C_\infty - \gamma_1 \exp(-\lambda_1 t) - \gamma_2 \exp(-\lambda_2 t)$, where $\beta_1 = [B'_0 - \lambda_2(B_\infty - B_0)]/(\lambda_1 - \lambda_2)$, $\beta_2 = [B'_0 - \lambda_1(B_\infty - B_0)]/(\lambda_2 - \lambda_1)$, $\gamma_1 = [C'_0 - \lambda_2(C_\infty - C_0)]/(\lambda_1 - \lambda_2)$, and $\gamma_2 = [C'_0 - \lambda_1(C_\infty - C_0)]/(\lambda_2 - \lambda_1)$. F_t can now be expressed in terms of the above parameters, $F_t = (AF_a + BF_b + CF_c)/\Gamma$, where $\Gamma = (A + B + C)$, from which

$$F_t = (A_\infty F_a + B_\infty F_b + C_\infty F_c)/\Gamma - (\alpha_1 F_a + \beta_1 F_b + \gamma_1 F_c) \times \exp(-\lambda_1 t)/\Gamma - (\alpha_2 F_a + \beta_2 F_b + \gamma_2 F_c) \exp(-\lambda_2 t)/\Gamma \quad (12)$$

Equation 12 is an expression that indicates the time course of fluorescence in systems described by the class of mechanisms in Scheme 4. For our purposes the parameter of most interest is F_r, that is, the ratio of the proportionality constants of terms $\exp(-\lambda_1 t)$ and $\exp(-\lambda_2 t)$:

$$F_r = (\alpha_1 F_a + \beta_1 F_b + \gamma_1 F_c)/(\alpha_2 F_a + \beta_2 F_b + \gamma_2 F_c)$$

From the above analysis of α_1, β_1, γ_1, α_2, β_2 and γ_2

$$F_r = -\{[A'_0 - \lambda_2(A_\infty - A_0)]F_a + [B'_0 - \lambda_2(B_\infty - B_0)]F_b + [C'_0 - \lambda_2(C_\infty - C_0)]F_c\}/\{[A'_0 - \lambda_1(A_\infty - A_0)]F_a + [B'_0 - \lambda_1(B_\infty - B_0)]F_b + [C'_0 - \lambda_1(C_\infty - C_0)]F_c\}$$

where $A'_0 = (-\kappa_{+1}A_0 + \kappa_{-1}B_0)$, $B'_0 = (\kappa_{+1}A_0 - \kappa_{-1}B_0 - \kappa_{+2}B_0 + \kappa_{-2}C_0)$, and $C'_0 = (\kappa_{+2}B_0 - \kappa_{-2}C_0)$. These expressions for A'_0, B'_0, and C'_0 are boundary conditions derived from $A' = (-\kappa_{+1}A + \kappa_{-1}B)$, etc. From this

$$F_r = -\{[-\kappa_{+1}A_0 + \kappa_{-1}B_0 - \lambda_2(A_\infty - A_0)]F_a + [\kappa_{+1}A_0 - \kappa_{-1}B_0 - \kappa_{+2}B_0 + \kappa_{-2}C_0 - \lambda_2(B_\infty - B_0)]F_b + [\kappa_{+2}B_0 - \kappa_{-2}C_0 - \lambda_2(C_\infty - C_0)]F_c\}/\{[-\kappa_{+1}A_0 + \kappa_{-1}B_0 - \lambda_1(A_\infty - A_0)]F_a + [\kappa_{+1}A_0 - \kappa_{-1}B_0 - \kappa_{+2}B_0 + \kappa_{-2}C_0 - \lambda_1(B_\infty - B_0)]F_b + [\kappa_{+2}B_0 - \kappa_{-2}C_0 - \lambda_1(C_\infty - C_0)]F_c\} \quad (13)$$

This expression for F_r (eq 13) can be related to mechanisms illustrated by Schemes 1, 5, and 7 or to experiments as set out in Scheme 2. For example, if we introduce the boundary conditions imposed in the calmodulin trapping experiment described by Scheme 2, and express Scheme 2 in terms of Scheme 4 where TA-cal is A, then $A_0 = 0$, $B_0 = \kappa_{-2}\Gamma/(\kappa_{+2} + \kappa_{-2})$, $C_0 = \kappa_{+2}\Gamma/(\kappa_{+2} + \kappa_{-2})$, $A_\infty = \Gamma$, $B_\infty = 0$, $C_\infty = 0$, and $\kappa_{+1} = 0$. Then, from eq 13

$$F_r = -\frac{(\kappa_{-1}\kappa_{-2} - \lambda_2\kappa_{+2} - \lambda_2\kappa_{-2})F_a + (\lambda_2\kappa_{-2} - \kappa_{-1}\kappa_{-2})F_b + \lambda_2\kappa_{+2}F_c}{(\kappa_{-1}\kappa_{-2} - \lambda_1\kappa_{+2} - \lambda_1\kappa_{-2})F_a + (\lambda_1\kappa_{-2} - \kappa_{-1}\kappa_{-2})F_b + \lambda_1\kappa_{+2}F_c} \quad (14)$$

In the Discussion, alternative mechanisms, Schemes 5 and 7, are compared to Scheme 1. A calmodulin trapping experiment to test Scheme 5 has the following boundary conditions in the context of Scheme 4: $A_0 = 0$, $B_0 = 0$, $C_0 = \Gamma$, $A_\infty = \kappa_{-1}\Gamma/(\kappa_{+1} + \kappa_{-1})$, $B_\infty = \kappa_{+1}\Gamma/(\kappa_{+1} + \kappa_{-1})$, $C_\infty = 0$, and $\kappa_{+2} = 0$. Then, from eq 13, we obtain the following expression for F_r:

$$F_r = -\{\lambda_2\kappa_{-1}F_a + (\lambda_2\kappa_{+1} - \kappa_{+1}\kappa_{-2} - \kappa_{-1}\kappa_{-2})F_b + (\kappa_{-2} - \lambda_2) \times (\kappa_{+1} + \kappa_{-1})F_c\}/\{\lambda_1\kappa_{-1}F_a + (\lambda_1\kappa_{+1} - \kappa_{+1}\kappa_{-2} - \kappa_{-1}\kappa_{-2})F_b + (\kappa_{-2} - \lambda_1)(\kappa_{+1} + \kappa_{-1})F_c\} \quad (15)$$

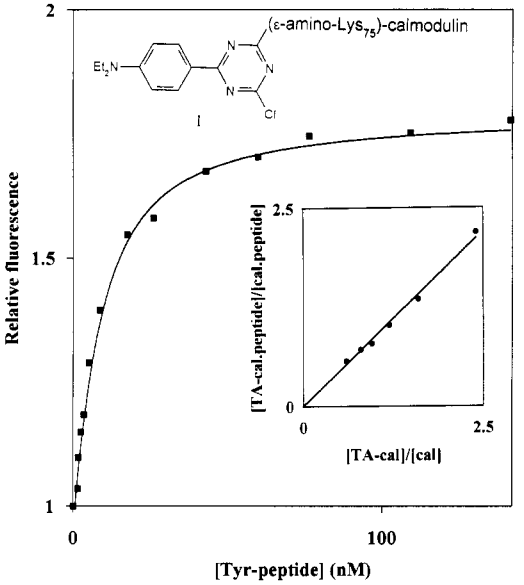

FIGURE 1: Equilibrium binding of TA-calmodulin (I) and calmodulin to Tyr peptide. (■) Aliquots of Tyr peptide were titrated into 11 nM TA-calmodulin and the fluorescence relative to the initial fluorescence was recorded. (λ_{ex} 365 nm, λ_{em} 410 nm). The nonlinear least-squares regression line to a simple equilibrium binding is drawn as a solid line through the data and gives the dissociation constant K_d = 6.3 (±0.3) nM. (●) To 100 nM Tyr peptide and 120 nM TA-calmodulin were added aliquots of calmodulin, so that the ratio of [TA-calmodulin] to [calmodulin] varied. From the fluorescence (λ_{ex} 365 nm, λ_{em} 410 nm), [TA-cal·Tyr peptide] and [TA-cal] and hence [cal·Tyr peptide] and [cal] were calculated. These data are plotted in the inset, and a linear regression line is drawn through them whose gradient (=0.875) is the ratio of K_d of Tyr peptide and calmodulin to K_d of Tyr peptide and TA-calmodulin.

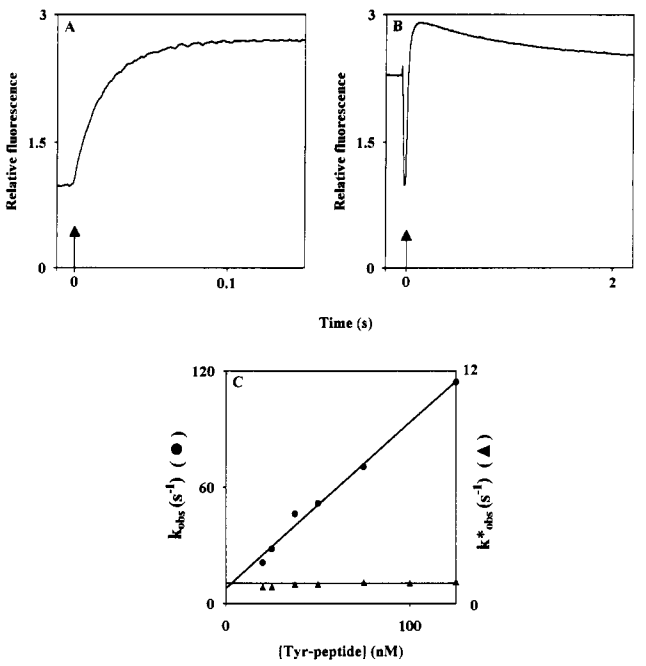

FIGURE 2: Association kinetics of TA-calmodulin and Tyr peptide. In panels A and B, 11.5 nM TA-calmodulin was mixed with 50 mM Tyr peptide (reaction chamber concentrations) in a stopped-flow fluorometer as described in Materials and Methods. Fluorescence records (λ_{ex} 365 nm, λ_{em} > 400 nm) are shown on two time scales. The time at which flow stops is taken as zero time and is marked by arrows. In panel A the fluorescence prior to zero time is of the solutions flowing in the mixing chamber. In panel B the extreme left-hand relative fluorescence is that of a preceding final reaction mixture. This is followed by a decrease of fluorescence during flow to that of panel A prior to zero time. In panel C, k_{obs} and k^*_{obs}, rate constants from the faster and slower exponential phases as seen in panels A and B, were plotted versus [Tyr peptide]. At 20 and 25 nM Tyr peptide, 5 nM TA-calmodulin was used. A linear regression line to the data (●) determines the gradient (=k_{+1}, eq 1) as 8.6 (±0.4) × 10^8 M^{-1} s^{-1} and the intercept as 8.0 (±2.9) s^{-1}. A horizontal line fitted to the data at >65 nM Tyr-peptide (▲) determines k^*_{obs} (= k_{+2} + k_{-2}, eq 2) as 0.99 (±0.06) s^{-1}. Below 65 nM Tyr peptide the condition $k_{+1}[P] \gg k_{-1}$ does not hold (i.e, the relative values are <10; see data in Figure 3). This topic is taken up in the Discussion.

The value of F_r derived from eq 15 is compared with the experimental data to find out whether Scheme 5 is a possible mechanism. A similar exercise can be undertaken for Scheme 7.

RESULTS

Equilibrium Binding of TA-Calmodulin and Calmodulin to Tyr Peptide. Figure 1 shows data obtained by titrating TA-calmodulin with Tyr peptide, from which a dissociation constant, K_d, of 6.3 (± 0.3) nM was determined. In the inset to Figure 1 are shown data obtained in an experiment in which the TA-calmodulin and calmodulin competed for peptide. From these data the ratio of the K_d of Tyr peptide to calmodulin to the K_d of Tyr peptide to TA-calmodulin was 0.875 (± 0.016), which leads to a K_d value of 5.5 (± 1.7) nM for calmodulin.

Association kinetics of TA-Calmodulin and Tyr Peptide. Figure 2 shows records obtained when TA-calmodulin and Tyr peptide were mixed in a stopped-flow fluorometer. The fluorescence transient was biphasic, and each phase could be analyzed as a single-exponential process. Rate constants k_{obs} and k^*_{obs} of the fast and slow phases were recorded as a function of peptide concentration and the data were analyzed in terms of Scheme 1 (Figure 2C). Data from two experiments led to averaged values for k_{+1} and (k_{+2} + k_{-2}) (Table 1).

Since $k_{obs} \gg k^*_{obs}$ for [P] > 50 nM, TA–calmodulin exists as TA-cal·P at the end of the faster phase for conditions where $k_{+1}[P] \gg k_{-1}$ (see Discussion and legend to Figure 2). It was thus possible to measure F_2 directly from the raw data. From these F_2 = 2.8 (normalized against F_1 = 1). On completion of the slower phase, the fluorescence amplitude F_∞ (eq 3) = 2.3. The ordinate intercept of the extrapolated linear plot of k_{obs} vs [P] is 8.0 s^{-1}, a result compatible with the expected value of the constant term in eq 1 which is approximately 5.7 s^{-1} from k_{-1} and the fact that k_{-1} is more than 5-fold greater than (k_{+2} + k_{-2}) (see next section and Table 1).

Dissociation Kinetics of TA-Calmodulin and Tyr Peptide. Figure 3A shows the fluorescence record when an excess of calmodulin was mixed with a solution of TA-calmodulin and Tyr peptide. Tyr Peptide was displaced from TA-calmodulin and, in terms of Scheme 2, the fluorescence decayed in a biphasic manner as described by eq 8. A least-squares fit to the data (see Materials and Methods and line 2 in Figure 3A) gives best-fit values for λ_1 and λ_2. Using (k_{+2} + k_{-2}) = 1.03 s^{-1} (Table 1) and eq 9 leads to values for k_{+2}, k_{-1}, and k_{-2} (legend to Figure 3). From the relative amplitudes of the two phases in Figure 3A (4.88) and eq 10, F_3 can be evaluated and equals 1.29. These results can now be fed into eq 3 to estimate F_∞ (=2.24), in agreement with the measurement of F_∞ (=2.3) determined from the association kinetics. Analysis of the data in Figures 2 and 3 also gives a second estimate of K_d, since K_d = $k_{-1}k_{-2}/k_{+1}(k_{+2} + k_{-2})$ = 4.1 nM. Results are summarized in Table 1.

We checked whether the biphasic association and dissociation kinetics of TA-calmodulin and Tyr peptide might have arisen because 100 μM Ca^{2+} was too low a concentration to saturate the Ca^{2+} binding sites on TA-calmodulin (Maune et al., 1992). Trials as described in Figures 2A,B and 3A were

Table 1: Parameters of the Tyr Peptide, Trp Peptide, and MLCK Interactions with TA-Calmodulin and Their Dissociation Constants with Calmodulin

	dissociation constants[a]		rate constants					relative fluorescence intensities		
	TA-calmodulin (nM)	calmodulin (nM)	k_{+1} (M^{-1} s^{-1})	$k_{+2} + k_{-2}$ (s^{-1})	k_{-1} (s^{-1})	k_{+2} (s^{-1})	k_{-2} (s^{-1})	F_1	F_2	F_3
Tyr peptide	4.1 (±0.4)[b]	3.6 (±0.4)	8.8 (±0.7) × 10^8	1.03 (±0.11)	5.7[c]	0.38[c]	0.65[c]	1	2.8	1.3
Trp peptide[d]	0.011 (±0.004)	0.006 (±0.002)	8.8 (±1.5) × 10^8	0.97 (±0.10)	0.01–0.1	0.25–0.92	0.08–0.75	1	2.2	0–1.6
MLCK	0.23–0.51	0.10–0.22	1.1 (±0.2) × 10^8	1.3 (±0.2)	0.56[e]	1.17[e]	0.13[e]	1	1.9	2.0

[a] Aqueous solution at 21 °C of 100 mM KCl, 100 μM $CaCl_2$, 2 mM $MgCl_2$, and 50 mM MES adjusted to pH 7.0 with KOH. [b] Standard deviations are listed. [c] These values were determined using $(k_{+2} + k_{-2}) = 1.03$ s^{-1} and eq 9, where $\lambda_1 = 6.16$ (±0.08) s^{-1} and $\lambda_2 = 0.61$ (±0.03) s^{-1}. [d] Monophasic dissociation of binary complex, so $k_{-1}k_{-2}/(k_{+2} + k_{-2}) = 0.0079$ (±0.0016) s^{-1}. Only ranges of values for k_{-1}, k_{+2}, k_{-2}, and F_3 could be determined (see text). [e] Best fit to experimental record of Figure 7.

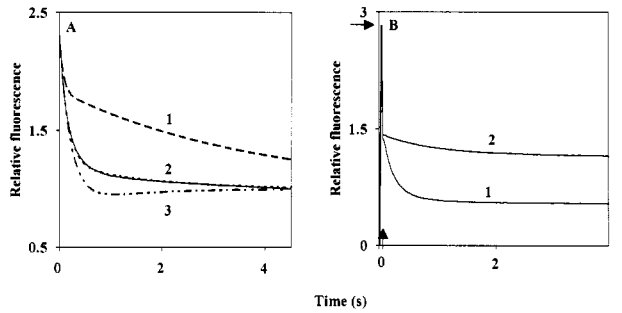

FIGURE 3: Displacement of Tyr peptide from TA-calmodulin by calmodulin. In panel A, 1.0 μM calmodulin was mixed with a solution containing 40 nM Tyr peptide and 20 nM TA-calmodulin. The solid line shows the fluorescence decay with time. The dashed line (2,- - -) overlying the data is the nonlinear least-squares fit of eq 8 to the data, which gives $\lambda_1 = 6.16$ (±0.8) s^{-1}, $\lambda_2 = 0.61$ (±0.03) s^{-1}, and the relative amplitude of the two phases (A_1/A_2) equals 4.88 (±0.12). From eq 9, $\lambda_1 + \lambda_2 = (k_{-1} + k_{+2} + k_{-2}) = (k_{-1} + 1.03)$ s^{-1}, and $\lambda_1\lambda_2 = k_{-1}k_{-2}$. It follows that $k_{+2} = 0.38$ s^{-1}, $k_{-1} = 5.7$ s^{-1}, and $k_{-2} = 0.65$ s^{-1}. As explained in the text, two simulations are drawn in which k_{+2} is set to 0.74 s^{-1} (line 1, – –) and 0.18 s^{-1} (line 3,–··–), respectively. [In the simulations there is no need to model the P trapping step (Scheme 2), as the preceding step (controlled by k_{-1}) is irreversible. This was checked by introducing an association rate constant of calmodulin (at 1 μM) to Tyr peptide of 8 × 10^8 M^{-1} s^{-1}. Doing this had no effect on the simulations.] In panel B, a double-mixing stopped-flow protocol was followed in which displacement of Tyr peptide from TA-calmodulin was examined prior to equilibration of the peptide and TA-calmodulin. TA-Calmodulin (50 nM) and Tyr peptide (100 nM) were mixed (concentrations in first mixing chamber), and after 55-ms delay at a time marked by the vertical arrow (zero time on abscissa), 2 μM calmodulin (trace 1) or buffer (trace 2) was mixed with this solution. The horizontal arrow shows the relative fluorescence just prior to the second mixing. The fluorescence drops by a factor of 2 as a consequence of dilution in the second mixing and then decreases further in both traces 1 and 2.

repeated in the presence of 1 mM rather than 100 μM Ca^{2+}. The records were unaffected by the change in $[Ca^{2+}]$. We investigated whether fluorescence transients arose when Tyr peptide was mixed with TA-calmodulin in the absence of Ca^{2+} (i.e., free $[Ca^{2+}] < 10^{-9}$ M). Trials as in Figure 2A,B were repeated in the presence of 20 mM EGTA with no added Ca^{2+}. No fluorescence changes occurred.

Also shown in Figure 3A are two simulations of Scheme 2 in which values of K_d, $(k_{+2} + k_{-2})$, F_1, F_2, and F_∞ (eq 3) are set to values (4.1 nM, 1.03 s^{-1}, 1, 2.8, and 2.3, respectively) determined from the data in Figures 2 and 3. In addition, k_{+2} is set to 0.74 s^{-1} (simulation, line 1) and 0.18 s^{-1} (simulation, line 3) (i.e., double and approximately half the estimated value of k_{+2}). This is turn leads to k_{-1}, k_{-2}, and, by using eq 3, F_3 values of 12.8 s^{-1}, 0.29 s^{-1}, and 2.11 and 4.4 s^{-1}, 0.85 s^{-1}, and 0.0, respectively. Both simulations diverge markedly from the actual data. This illustrates that the rate constants in Scheme 1 are rather rigorously constrained by the data and that the equilibrium constant of the isomerization (k_{+2}/k_{-2}) has a value close to 0.58.

As explained in Design and Theory of Kinetic Experiments, the double-mixed stopped-flow experiment described in Figure 3B provided information about the fate of the intermediate TA-cal·P (Scheme 3). In view of the greater value of k_{-1} compared to k_{+2} and the irreversible nature of the calmodulin trapping, it is not surprising that the fluorescence decay in trace 1 of Figure 3B approximates to the decay seen in Figure 3A. Also, if buffer is added on the second mixing (Figure 3B, trace 2), the fluorescence record, as expected, continues much as it does 55 ms after mixing in Figure 2B. The relevance of this experiment is in the contrast of its result to that obtained when Trp peptide replaced Tyr peptide (Figure 5C).

Equilibrium Binding of TA-Calmodulin and Calmodulin to Trp Peptide. TA-Calmodulin (11 nM) was titrated with Trp peptide following the protocol described in Figure 1. The fluorescence first increased 1.92-fold linearly with [Trp peptide] to approximately 1:1 stoichiometry. The data suggested high-affinity binding for which an upper limit of 1 nM could be placed on the value of K_d. Kinetic analysis (see below and Table 1) confirmed this result. On titrating in further Trp peptide, the fluorescence decreased so that the overall increase was 1.72-fold. The data could be interpreted in terms of an additional Trp peptide binding site on TA-calmodulin but the results were variable, giving K_d values in the range 5–50 nM of indeterminate stoichiometry. We have not explored this possible additional peptide binding site. However, we did check carefully to see whether any fluorescence changes arose from this secondary binding in our transient kinetic experiments whose primary focus was exploration of the high-affinity TA-calmodulin·Trp peptide interaction.

A competition experiment between TA-calmodulin and calmodulin for Trp peptide was carried out as described for the Tyr peptide (legend to Figure 1). Only the high-affinity binding site was involved since the total ([TA-calmodulin] + [calmodulin]) was greater than [Trp peptide]. From the data (not shown), the ratio of the K_d of Trp peptide and calmodulin to the K_d of Trp peptide and TA-calmodulin was 0.52. This leads to a K_d of 0.006 nM for calmodulin based on the kinetically determined K_d of 0.011 nM for TA-calmodulin (see below and Table 1).

Association Kinetics of TA-Calmodulin and Trp Peptide. Figure 4A shows a record when TA-calmodulin and Trp peptide were mixed in a stopped flow fluorometer. The record is similar in appearance to corresponding records obtained with Tyr peptide as in Figure 2B. Rate constants k_{obs} and k^*_{obs} of the fast and slow phases were recorded as a function of peptide concentration and the data were analyzed in terms of Scheme 1 (Figure 4C). Data from three experiments lead to averaged values for k_{+1} and $(k_{+2} + k_{-2})$ (Table 1). A

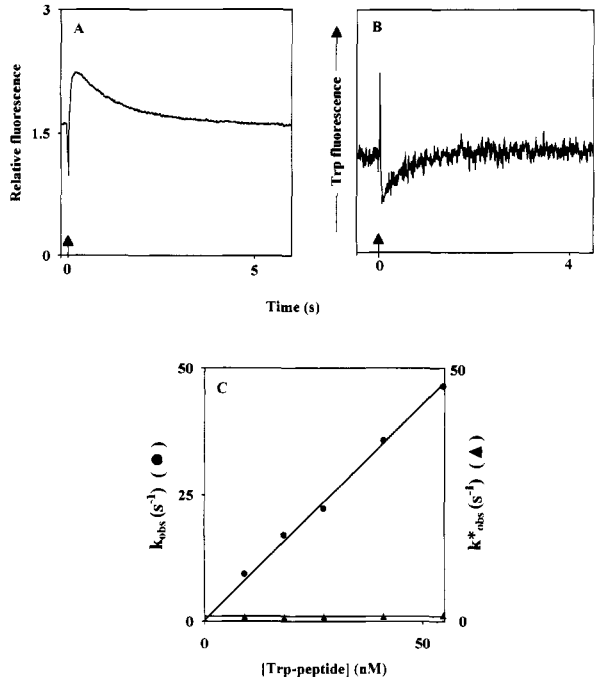

FIGURE 4: Association kinetics of TA-calmodulin and Trp peptide. In panel A, 5 nM TA-calmodulin was mixed with 55 nM Trp peptide (concentrations in reaction chamber) as described in the legend to Figure 2. In panel B, 6.6 μM TA-calmodulin was mixed with 10 μM Trp peptide. The fluorescence record (λ_{ex} 290 nm, λ_{em} 350 nm) is shown. In panels A and B the time at which flow stops is marked by arrows (zero time on abscissa). In panel C, k_{obs} and k^*_{obs}, rate constants for the faster and slower exponential phases seen in panel A, were plotted versus [Trp peptide]. A linear regression line to the data (●) determines the gradient ($=k_{+1}$, eq 1) as 8.2 (±0.3) × 10^8 M^{-1} s^{-1}. A best-fit horizontal line to the data (▲) determines k^*_{obs} ($=k_{+2} + k_{-2}$, eq 2) as 0.93 (±0.07) s^{-1}.

control experiment with Trp peptide in the absence of Ca^{2+} was done as described above for Tyr peptide. No fluorescence changes occurred when trials as in Figure 4A were repeated in 20 mM EGTA with no added Ca^{2+}.

Figure 4B shows a transient change of fluorescence at 350 nm (λ_{ex} 290 nm) when Trp peptide was mixed with TA-calmodulin. Micromolar reagent concentrations were required to detect the change, thus limiting measurement of the bimolecular association because of the time resolution of the stopped-flow apparatus. We ascribe the exponential process at 1.7 s^{-1} to Trp fluorescence. The fluorescence increase contrasts with the decrease in the TA fluorescence occurring over the same time range (Figure 4A). The fluorescence change may be due to energy transfer and/or the conformational change. In any event it is likely that probes on both Trp peptide and TA-calmodulin are responding to the interaction. This is not surprising in view of the known sensitivity of Trp fluorescence to MLCK or MLCK-derived peptides binding to calmodulin (Kasturi et al., 1993; Lukas et al., 1986).

To this point we have analyzed the kinetic data on the premiss that the observed fluorescence changes are associated with formation of a 1:1 TA-calmodulin·Trp peptide complex. However, equilibrium binding data described above indicated that multiple (two or more) peptide molecules may bind per TA-calmodulin molecule. In order to check that the biphasic fluorescence change (Figure 4A) is associated, at least predominantly, with 1:1 complex formation, Trp peptide was mixed with TA-calmodulin in excess. An identical fluorescence time course was observed within the limits of experimental accuracy for up to 100 μM reactant concentrations

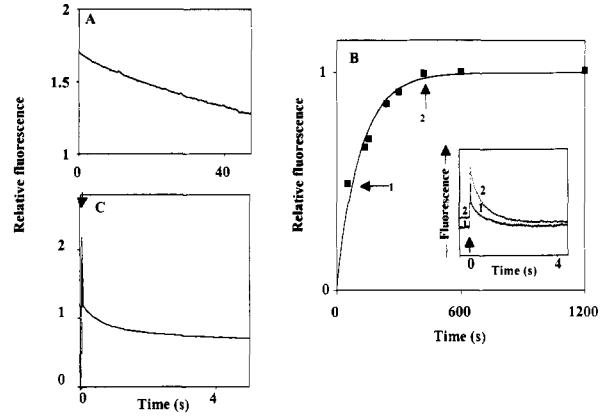

FIGURE 5: Displacement of Trp peptide from TA-calmodulin by calmodulin. Panel A shows the initial phase of the displacement when 2.0 μM calmodulin was mixed with a solution containing 50 nM Trp peptide and 10 nM TA-calmodulin. The solid line shows the fluorescence decay with time. Assuming that the fluorescence end point corresponded to the fluorescence of free TA-calmodulin and that the fluorescence decayed exponentially, then the observed rate constant was 0.0075 (±0.0004) s^{-1}. In panel B, a double-mixing stopped-flow protocol was followed to circumvent photobleaching that occurs during long exposure to the exciting light. An equilibrated mixture of 50 nM TA-calmodulin and 100 nM Trp peptide was first rapidly mixed with 4 μM calmodulin (concentrations in the reaction chamber after the first mixing with 25 nM TA-calmodulin, 50 nM Trp peptide, and 2 μM calmodulin). The free TA-calmodulin generated by displacement of Trp peptide over a period of time was measured in a second mixing step with excess (10 μM) Trp peptide. The amplitude of the fluorescence change in this reaction (corresponding to the slower phase in Figure 4A), was determined at various time points. In a control experiment (that defined zero relative fluorescence at zero time), calmodulin was absent and buffer alone was used in one of the stopped-flow syringes at the first mixing. The inset (with the arrow marking the second mixing time) shows the fluorescence change of displaced TA-calmodulin as it interacts with excess Trp peptide at two selected time points (1 and 2 in main data set). A best-fit exponential decay is drawn through the data points with the end point (not shown) being determined by the amplitude of the fluorescence change when there was 300 min between the first and second mixing. The amplitude of the fluorescence changes is plotted relative to that obtained from the end point. k_{diss} for TA-calmodulin dissociation from Trp peptide determined by the exponential release of TA-calmodulin was 0.0082 (±0.0012) s^{-1}. In panel C, a second double-mixing stopped-flow protocol was followed as in Figure 3B. TA-Calmodulin (20 nM) and Trp peptide (200 nM) were mixed (concentrations in the first mixing chamber) and after 40-ms delay at a time marked by the arrow on top of the frame (zero time on abscissa), 20 μM calmodulin was mixed with this solution. The left-hand side of the panel shows the fluorescence change of TA-calmodulin between the first and second mixing. This fluorescence initially increases upon Trp peptide binding followed by a decrease as a consequence of dilution in the second mixing. A further decrease of fluorescence then follows.

(data not shown). However, the somewhat faster process (1.7 s^{-1}) shown in Figure 4B compared to k^*_{obs} from Figure 4C (0.93 s^{-1}) suggests that the kinetics may be influenced by secondary binding of Trp peptide at the micromolar concentrations of the experiment. To summarize, the data of Figures 2 and 4 indicate that Tyr peptide and the tighter binding molecule of Trp peptide interact with TA-calmodulin by a similar two-step mechanism.

Dissociation Kinetics of TA-Calmodulin and Trp Peptide. The dissociation of the TA-calmodulin·Trp peptide complex was analyzed in two ways. The complex was mixed with an excess of calmodulin so that the peptide was sequestered as it dissociated from TA-cal. The observed fluorescence change was monophasic (Figure 5A). To check for possible interference from multiple Trp peptide binding, the experiment was repeated with TA-calmodulin (22 nM) in excess of Trp peptide (16 nM). The time course of the fluorescence change was

identical to that in Figure 5A. If a fluorescence end point for the record in Figure 5A was assumed to be equal to the fluorescence of free TA-calmodulin, and it was further assumed that the fluorescence decayed exponentially, then the rate constant of dissociation k_{diss} = 0.0075 s^{-1}. Some photobleaching occurred during the decay, as indicated in the legend to Figure 5. To avoid this problem and measure the time course of the later part of the reaction, a double-mixing stopped-flow experiment was set up as indicated in the legend to Figure 5B. The best fit to these data gave k_{diss} = 0.0082 s^{-1}. The mean of these values (0.0079 s^{-1}) was taken to be the value of k_{diss} (Table 1).

These dissociation data differ markedly from those observed with the TA-calmodulin·Tyr peptide complex and could be treated according to eqs 6 and 7. The monophasic response in the dissociation coupled with the biphasic association suggests that, in terms of Schemes 1 and 2 and eq 6, $k_{diss} = k_{-1}k_{+2}/(k_{+2} + k_{-2})$ and that either $k_{+2} \gg k_{-2}$, $k_{+2} \approx k_{-2} \gg k_{-1}$, or $k_{+2} \gg k_{-1}$ and k_{-2}. A double-mixing stopped-flow experiment was carried out to probe the mechanism further by investigating the properties of the intermediate TA-cal·P (Figure 5C). Calmodulin was added at the second mixing and the time course of the fluorescence decay was essentially the same as it would have been if buffer had been added (i.e., the fluorescence time course observed after 40 ms in Figure 4A). So in contrast to the case with the Tyr peptide, when calmodulin is added to TA-cal·P (where P is Trp peptide), the reaction proceeds to TA-cal·P*. Only on a much slower time scale is P displaced as in Figure 3A. Thus $(k_{+2} + k_{-2}) \gg k_{-1}$ and therefore $k_{-1} < 0.1$ s^{-1}.

We then attempted to place limits on rate constants k_{+2} and k_{-2}. For this we used the fact that the fluorescence of each TA-calmodulin species cannot have a negative value. The relative fluorescence intensities F_1, F_2, and F_∞ of TA-cal, TA-cal·P, and the equilibrium mixture of TA-cal·P and TA-cal·P* (Scheme 1, eq 3) were estimated relative to one another from association kinetic experiments as in Figure 5A. The problem of secondary Trp peptide binding was avoided by carrying out the experiments with [Trp peptide] < [TA-calmodulin]. By definition F_1 = 1, and F_2 = 2.2 from the fluorescence amplitude at the peak of the transient because at that time essentially all TA-calmodulin existed as TA-cal or TA-cal·P. The final fluorescence allowed evaluation of F_∞ as 1.64. Now $F_3 > 0$ and, using eq 3, $1.64 = (\delta\ k_{+2} + 2.2\ k_{-2})/(k_{+2} + k_{-2})$, where δ is a positive number. So $k_{+2}/k_{-2} > 0.35$, and as $(k_{+2} + k_{-2})$ = 0.97 s^{-1}, it follows that $0.25 < k_{+2} < 0.97$ s^{-1} and $0 < k_{-2} < 0.72$ s^{-1}. Since $k_{diss} = k_{-1}k_{-2}/(k_{+2} + k_{-2})$ = 0.0079 s^{-1} and $(k_{+2} + k_{-2})$ = 0.97 s^{-1}, $k_{-1}k_{-2}$ = 0.0077 s^{-2}. We also know from the previous paragraph that $k_{-1} < 0.1$ s^{-1}, so $k_{-2} > 0.077$ s^{-1}. It then follows that $0.077 < k_{-2} < 0.72$ s^{-1} and $0.25 < k_{+2} < 0.87$ s^{-1}. We can further refine limits of k_{-1}. Since $k_{-1} = 0.0077/k_{-2}$ s^{-1} and $k_{-2} < 0.72$ s^{-1}, $0.01 < k_{-1} < 0.1$ s^{-1}. This analysis is summarized in Table 1. Defining the rate constants further requires an additional measurement, for example, the relative concentrations of TA-cal·P and TA-cal·P* at equilibrium.

Equilibrium Binding of TA-Calmodulin and Calmodulin to MLCK. TA-Calmodulin (4.6 nM) was titrated with MLCK following the protocol described in Figure 1. The result was similar to that obtained with Trp peptide in that the data were consistent with formation of a TA-calmodulin·MLCK complex of high affinity (K_d < 1 nM) and this complex had fluorescence intensity 1.85-fold that of TA-calmodulin. Kinetic analysis (see below and Table 1) confirmed this result. On titrating in more MLCK, the fluorescence increased by a further 10%.

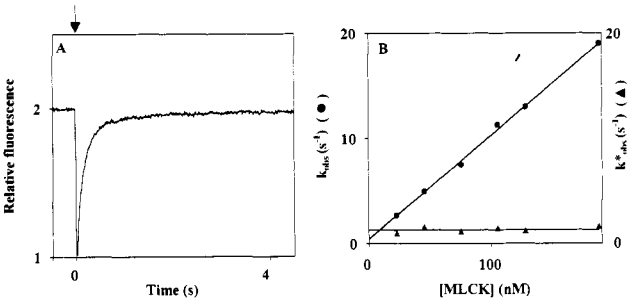

FIGURE 6: Association kinetics of TA-calmodulin and MLCK. In panel A, 2.5 nM TA-calmodulin was mixed with 75 nM MLCK (concentrations in mixing chamber) as described in the legend to Figure 2. The time at which flow stops is marked by an arrow (zero time on abscissa). In panel B, k_{obs} and k^*_{obs}, rate constants for the faster and slower exponential phases seen in panel A, were plotted versus [MLCK]. A linear regression line to the data (●) determines the gradient ($=k_{+1}$, eq 1) as 0.99 (±0.02) × 10^8 M^{-1} s^{-1}. A best-fit horizontal line to the data (▲) determines k^*_{obs} ($=k_{+2} + k_{-2}$, eq 2) as 1.3 (±0.2) s^{-1}.

No attempt was made to characterize this additional fluorescence change that was most readily explained as being due to lower affinity interactions of indeterminate stoichiometry between MLCK and the TA-calmodulin·MLCK complex (cf. Trp peptide).

A competition experiment between TA-calmodulin and calmodulin for MLCK was carried out as described by Tyr peptide (legend to Figure 1) and Trp peptide. From these data (not shown) the ratio of the K_d of MLCK and calmodulin to the K_d of MLCK and TA-calmodulin was 0.43. This leads to a K_d of 0.10–0.22 nM for calmodulin based on the kinetically determined K_d of 0.23–0.51 nM for TA-calmodulin (see below and Table 1).

Association Kinetics of TA-Calmodulin and MLCK. Figure 6A shows a record when TA-calmodulin and MLCK were mixed in a stopped-flow fluorometer. The record is similar to corresponding records obtained with Tyr peptide and Trp peptide (Figures 2B and 4A) in that it is biphasic but is dissimilar in that the slower phase occurs with an increase in fluorescence. Rate constants k_{obs} and k^*_{obs} of the fast and slow phases were recorded as a function of MLCK concentration and the data were analyzed in terms of Scheme 1 (Figure 6B). Averaged data led to values for k_{+1}, $(k_{+2} + k_{-2})$, F_2, and F_∞ (Table 1).

Dissociation Kinetics of TA-Calmodulin and MLCK. Figure 7A shows a fluorescence record when an excess of calmodulin was mixed with a solution of TA-calmodulin and MLCK. The fluorescence decay that accompanied the MLCK dissociation was monophasic. About 10% of the change was due to photobleaching and the record in Figure 7A is corrected for this. The decay could be described approximately by a single exponential from which k_{diss} = 0.031 s^{-1}. Over several trials significant variation occurred, probably due in part to the photobleaching. The range of values for k_{diss} was 0.025–0.056 s^{-1}, so that in terms of Scheme 2, $k_{-1}k_{-2}/(k_{+2} + k_{-2})$ = 0.025–0.056 s^{-1} (eq 6) and K_d = 0.23–0.51 nM.

A double-mixing stopped-flow experiment was carried out in which TA-calmodulin was mixed with MLCK and this solution was then further mixed with excess calmodulin. The experiment permits analysis of the properties of the TA-calmodulin·MLCK intermediate corresponding to TA-cal·P in Scheme 3. The fluorescence records (Figure 7B) are analogous to those illustrated in Figures 3B and 5C involving Tyr peptide and Trp peptide, except that the recordings were made from the times of the second mixing (100 ms in record

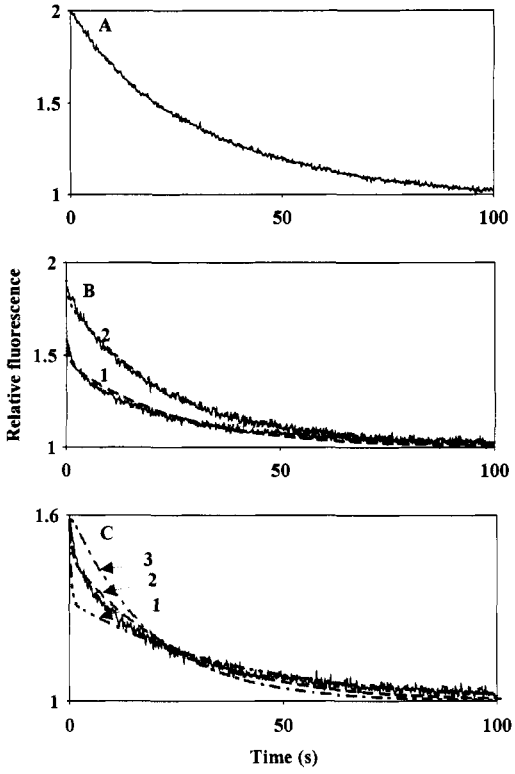

FIGURE 7: Displacement of MLCK from TA-calmodulin by calmodulin. Panel A shows the displacement when 1.0 μM calmodulin was mixed with a solution containing 45 nM MLCK and 10 nM TA-calmodulin. Fluorescence decay was approximately a single exponential at 0.031 s^{-1}. In panel B, a double-mixing stopped-flow protocol was followed as in Figure 3B. TA-Calmodulin (5 nM) and MLCK (200 nM) were mixed (concentrations in the first mixing chamber), and after set delays (100 ms in record 1 and 500 ms in record 2), this solution was mixed with calmodulin. Final protein concentrations in the second mixing chamber were 2.5 nM TA-calmodulin, 100 nM MLCK, and 3.5 μM calmodulin. The records showed biphasicity for which the experimental fits (see Materials and Methods) are as follows: record 1, $\lambda_1 = 0.31$ s^{-1} and $\lambda_2 = 0.032$ s^{-1}, with relative amplitude of the two phases being 0.39; record 2, $\lambda_1 = 0.18$ s^{-1} and $\lambda_2 = 0.033$ s^{-1}, with relative amplitude of the two phases being 0.26. The dotted lines that overlay the experimental records are simulations of Scheme 2 using $k_{-1} = 0.56$ s^{-1}, $k_{+2} = 1.17$ s^{-1}, $k_{-2} = 0.13$ s^{-1}, and $F_3 = 2.01$, values for the best fit of eq 7 to the data. [TA-cal], [TA-cal·P], and [TA-cal·P*] at zero time were required for the simulations. These were obtained by simulating the association of 5 nM TA-cal and 200 nM P and evaluating [TA-cal], [TA-cal·P], and [TA-cal·P*] at 100 ms (simulation 1) and 500 ms (simulation 2). As described in the legend to Figure 3, there was no need to model the final trapping step, as the process controlled by k_{-1} is irreversible in Scheme 2. Both simulations show a significantly faster inital phase than expected from the values of λ_1. This discrepancy is discussed in the text. In panel C, additional simulations are shown that relate to record 1 in panel B that is shown as the solid line with its ordinate scale expanded compared to that in panel B. As explained in the text, three simulations are drawn in which k_{+2}/k_{-2} and F_3 are set to 25 and 2.00 (line 1,—··—), 9 and 2.01 (line 2,– – –), and 1 at 2.10 (line 3,– · –), respectively. $k_{-1}k_{-2}/(k_{+2} + k_{-2}) = 0.056$ s^{-1} and $(k_{+2} + k_{-2}) = 1.3$ s^{-1} throughout.

1; 500 ms in record 2). Record 1 has pronounced biphasic character. In terms of Scheme 3, the first phase of fluorescence decay is dominated by the dissociation of P from TA-cal·P and the second phase by the isomerization of TA-cal·P* to TA-cal·P followed by dissociation of P. This behavior is in contrast to that seen in Figure 7A and is presumably due to the differing ratios of [TA-cal·P] to [TA-cal·P*] at the time of adding excess calmodulin.

Analysis of the biphasic data in Figure 7B (shown with expanded ordinate in Figure 7C) was more complicated than in the dissociation experiments involving Tyr or Trp peptide

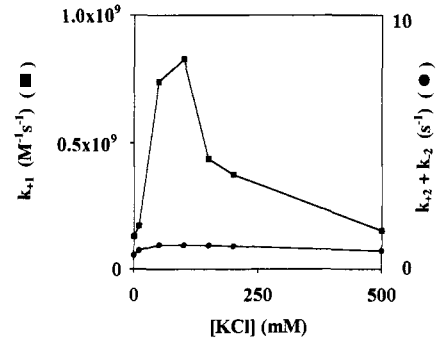

FIGURE 8: Dependence of the kinetics of TA-calmodulin and Trp peptide association on KCl concentration. TA-Calmodulin (5 nM) was mixed with 55 nM Trp peptide as described for Figure 4A except that [KCl] was varied as indicated and [Ca^{2+}] was 1 mM. In the absence of KCl the ionic strength was 0.05 M. k_{+1} (■) and $(k_{+2} + k_{-2})$ (●) were calculated from the faster and slower phases of the observed fluorescence change (see text) and plotted vs [KCl].

(Figures 3 and 5). In the latter cases best fits of either double or single exponentials to the data were readily accommodated by the other data (Figures 1, 2, and 4). The difficulty here is that if the data are fitted as was done in Figure 3A, an inconsistency arises as follows. From eq 9, $(\lambda_1 + \lambda_2) = (k_{-1} + k_{+2} + k_{-2})$ and from Figure 6 $(k_{+2} + k_{-2}) = 1.3$ s^{-1}, so that $(\lambda_1 + \lambda_2) > 1.3$ s^{-1}. However, the best fit to the data gives $(\lambda_1 + \lambda_2) = 0.34$ s^{-1} (i.e., $k_{-1} < 0$!).

The alternative we have adopted is to simulate time courses for records 1 and 2 in Figure 7B that are compatible with the data of Figure 6 and are otherwise a best fit to the observed MLCK dissociation records. Values for k_{-1}, k_{+2}, k_{-2}, and F_3 obtained in this way are listed in Table 1. The fit to the data using these values is shown in simulation 2 of Figure 7C. Other simulations are shown in which $k_{+2}/k_{-2} = 25$ (simulation, line 1) and $k_{+2}/k_{-2} = 1$ (simulation, line 3). These diverge widely from the data and simulation, line 2, in which $k_{+2}/k_{-2} = 9$. In all three simulations $k_{-1}k_{-2}/(k_{+2} + k_{-2})$ was set of 0.056 s^{-1} and $(k_{+2} + k_{-2})$ to 1.3 s^{-1}. In conclusion, there is considerable uncertainty concerning the individual rate constants k_{-1}, k_{+2}, and k_{-2} associated with the TA-calmodulin·MLCK interaction. The values listed in Table 1 are the most plausible estimates.

Dependence of the Association Kinetics on KCl Concentration. The second-order rate constant of association of TA-calmodulin with each of the three target molecules is diffusion-controlled and among the fastest recorded for a protein–ligand or protein–protein association. Here we investigated the dependence of the reaction rate on [KCl] in an attempt to learn about the physical chemistry of the interactions involved in the process. The rate of the fluorescence change that occurs when TA-calmodulin was mixed with Trp peptide was measured as a function of [KCl] and interpreted as yielding values for k_{+1} and $(k_{+2} + k_{-2})$ (Figure 8 and eqs 1 and 2, with the constant set to zero in eq 1). One millimolar rather than 100 μM Ca^{2+} was used to minimize the amount of calmodulin not fully saturated with Ca^{2+}, since calmodulin is not quite fully saturated at 100 μM Ca^{2+} (Maune et al., 1992). If it is assumed that a similar first-order dependence of k_{obs} on [Trp peptide] occurs over the range of [KCl] studied and that the effect is not K^+- or Cl^--specific, then inferences can be made about the influence of ionic strength on the interaction of TA-calmodulin and Trp peptide.

DISCUSSION

How Valid Are the Experimental Results? The results reported here are striking in that some properties of the

interaction of TA-calmodulin with its targets are common to all three studies while others are quite diverse. It is important to comment on which results can be confidently used to define mechanisms and which ones should be treated more cautiously.

We have defined precisely the composition of TA-calmodulin with respect to molecular homogeneity and specificity of labeling and checked that Tyr peptide and Trp peptide are single molecular species. These are essential steps in establishing mechanisms based on the amplitudes and kinetics of fluorescence changes. While the homogeneity of MLCK has not been established with the same degree of confidence, it runs as a single band in SDS–PAGE and has satisfactory specific activity of 4.8 μmol of MLC phosphorylation·min^{-1}·(mg of MLCK)$^{-1}$ at 22 °C and pH 7.0 in the presence of 120 nM calmodulin (data not shown).

One property of the systems that complicates analysis is the influence of weak interactions evident between TA-calmodulin·Trp peptide and Trp peptide and between TA-calmodulin·MLCK and MLCK. By carrying out control experiments with excess TA-calmodulin, we have minimized potential artifacts arising from this property.

As pointed out in the Results, one conclusion that should be treated with caution is the estimate of discrete values for k_{-1}, k_{+2}, and k_{-2} in the TA-calmodulin interaction with MLCK. However, the estimated range of values for $k_{-1}k_{-2}/(k_{+2} + k_{-2})$, on which the K_d values of TA-calmodulin and calmodulin for MLCK depend, is reliable. All the other results listed in Table 1 we consider may be used with confidence in helping define mechanism.

Discrimination against Alternative Mechanisms of the Interaction of TA-Calmodulin and Tyr Peptide. We first consider possible alternative two-step mechanisms to Scheme 1 for protein–ligand interactions and relate them to our kinetic results. Mechanisms in which either the protein or ligand isomerizes prior to the association step are generally not easy to discriminate from mechanisms in which the isomerization occurs after the association, as in Scheme 1 (Fersht, 1984; Gutfreund, 1972). Even so, there are several examples (Bagshaw et al., 1974; Fersht & Requena, 1971; Halford, 1971, 1972; Kirschner et al., 1966) where distinct pathways have been resolved or partially resolved, generally by use of rapid mixing or relaxation techniques. In the case of the interaction of TA-calmodulin and Tyr peptide, alternative mechanisms to Scheme 1 can be eliminated (or at most be designated a minor pathway) by qualitative as well as quantitative arguments about the amplitudes of the fluorescence changes in the transient experiments (Figures 2 and 3). In terms of Scheme 1 this is because of the remarkably high fluorescence intensity of the intermediate TA-cal·P ($F_2 = 2.8$) compared to that of TA-cal and TA-cal·P* and because the equilibrium constant between TA-cal·P and TA-cal·P* is poised close to unity.

Scheme 5

$$\text{TA-cal} \underset{k'_{-1}}{\overset{k'_{+1}}{\rightleftharpoons}} \text{TA-cal*} + \text{P} \underset{k'_{-2}}{\overset{k'_{+2}}{\rightleftharpoons}} \text{TA-cal·P*}$$

Consider first a mechanism (Scheme 5) in which TA-cal isomerizes prior to the binding of P in relation to the data of Figures 2 and 3. [To make such a scheme conceptually tangible, one may consider TA-cal and TA-cal* as being related to the two structures of $CAPP_1$-calmodulin in which the norchlorpromazine group can associate with approximately equal probability with the C- and N-terminal hydrophobic patches of calmodulin (Newton & Klee, 1989).] When excess Tyr peptide (P) is mixed with TA-calmodulin (comprising TA-cal and TA-cal*), P will react rapidly with TA-cal* in a bimolecular step. This will be followed by isomerization of TA-cal and further binding of P to newly formed TA-cal* so that ultimately all the TA-calmodulin is converted to TA-cal·P*. From the record of bimolecular association (Figure 2A), the fluorescence of TA-cal·P* is greater than that of TA-cal*. From the isomerization step (Figure 2B), the fluorescence of TA-cal is greater than that of TA-cal·P*. It follows that the fluorescence of TA-cal is greater than that of TA-cal*. Consider now the dissociation (as described in Figure 3) and what happens when TA-cal·P* forms TA-cal* and P that is immediately trapped by calmodulin. Initially the fluorescence will fall because TA-cal* is formed and the fluorescence of TA-cal·P* is greater than that of TA-cal*. This is observed (Figure 3A). Then the fluorescence will *increase* because TA-cal is formed from TA-cal* in the second step of the dissociation and the fluorescence of TA-cal is greater than that of TA-cal*. This is contrary to what is observed (slower phase, Figure 3A), so that the mechanism described by Scheme 5 is untenable.

Scheme 6

$$\text{P} \underset{k'_{-1}}{\overset{k'_{+1}}{\rightleftharpoons}} \text{P*} + \text{TA-cal} \underset{k'_{-2}}{\overset{k'_{+2}}{\rightleftharpoons}} \text{TA-cal·P*}$$

A further alternative mechanism (Scheme 6) is that in which P isomerizes prior to binding to TA-cal. In this case when Tyr peptide (comprising P and P*) is mixed with TA-calmodulin (TA-cal), P* will react rapidly with TA-cal in a bimolecular step. This will be followed by an isomerization of P and, if TA-camodulin is not already saturated, by further binding of TA-cal to newly formed P*, so that ultimately all the protein is converted to TA-cal·P*.

This mechanism is, however, incompatible with the fluorescence changes in the association experiment (Figure 2). In the bimolecular step the fluorescence increases; therefore, in terms of Scheme 6, the fluorescence of TA-cal·P* is greater than that of TA-cal. If at this point TA-calmodulin is saturated, the reaction will be a single exponential, a result incompatible with the data. Therefore we must presume TA-calmodulin is not saturated. Following the isomerization, more TA-cal·P* is formed from TA-cal so that fluorescence must *increase* further. But this is not observed (Figure 2B), so that the mechanism described by Scheme 6 is also untenable.

Simulations of the transient fluorescent changes provide a quantitative description of how the kinetic data illustrated in Figures 2 and 3 would appear if the isomerization of TA-cal occurred prior to P binding (Scheme 5). Rate constants for the simulations were derived from the data in Figures 2 and 3 and are as follows: $k'_{+1} = 0.65\ s^{-1}$; $k'_{+2} = 8.8 \times 10^8\ M^{-1}\ s^{-1}$; $k'_{-1} = 0.38\ s^{-1}$; $k'_{-2} = 5.7\ s^{-1}$. First a simulation was made of the association data to obtain the best fit for the fluorescence amplitudes of TA-cal, TA-cal*, and TA-cal·P*. The amplitudes of the fluorescence changes could only be made approximately compatible with the association data; the problem is that, to be fully consistent, the normalized initial fluorescence (defined by $F'_1 = 1$) derives from TA-cal and TA-cal*, the normalized intermediate peak fluorescence (F'_i) is 2.8 and derives from TA-cal and TA-cal·P*, and the final fluorescence is 2.3. This leads to a negative value for F'_2 (the fluorescence of TA-cal*) of –0.5, which is impossible. Nevertheless, a simulation approximately consistent with the data is obtained if F'_i is lowered to 2.5 so that $F'_1 = 0.9\ F'_i = 2.5$, $F'_2 = 0$, and the fluorescence of TA-cal·P*, F'_3, is 2.3.

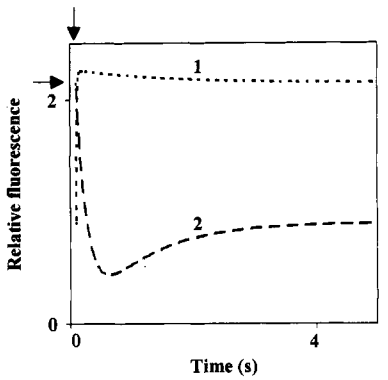

FIGURE 9: Simulations of TA-calmodulin interaction with Tyr peptide. In the simulation shown by line 1 (- - -), 20 nM TA-calmodulin was mixed with 100 nM Tyr peptide and the time course shows the fluorescence change according to Scheme 5 with the following parameters: $k'_{+1} = 0.65\ s^{-1}$, $k'_{+2} = 8.8 \times 10^8\ M^{-1}\ s^{-1}$, $k'_{-1} = 0.38\ s^{-1}$, $k'_{-2} = 5.7\ s^{-1}$, $F'_1 = 0.9$, $F'_i = 2.5$, $F'_2 = 0$, and $F'_3 = 2.3$. In the simulation shown by line 2 (– – –), 20 nM TA-calmodulin·Tyr peptide complex was mixed with calmodulin to trap Tyr peptide as it was formed (i.e., k_{+2}[P] set to zero), and the time course shows the fluorescence change according to Scheme 5 with the same parameters as in line 1. The horizontal arrow indicates the relative fluorescence of line 2 at zero time. The vertical arrow marks time of mixing (zero time on abscissa).

The fluorescence at the end of the association is then 2.15 (Figure 9), not 2.3, because at the final equilibrium small (relative to TA-cal·P*) amounts of TA-cal and TA-cal* are present. Simulation of the time course of the fluorescence change on dissociation of P from TA-cal·P* by calmodulin trapping in accordance with Scheme 5 passes through a minimum (Figure 9), unlike what is observed (Figure 3).

In terms of eq 15, values for F_a, F_b, and F_c used in the simulation are $F_a = 2.5$, $F_b = 0$, $F_c = 2.3$, $\kappa_{+1} = 0.65\ s^{-1}$, $\kappa_{-1} = 0.38\ s^{-1}$, and $\kappa_{-2} = 5.7\ s^{-1}$, from which $\lambda_1 = 5.7\ s^{-1}$ and $\lambda_2 = 1.03\ s^{-1}$ (by use of eq 11 with $\kappa_{+2} = 0$). When these are substituted into eq 15 we obtain $F_r = -2.22$. The negative sign confirms the nature of the simulation (Figure 9, line 2), a biphasic reaction in which the fluorescence changes direction. Calculation of the minimum value of F_t (i.e., when $dF_t/dt = 0$) using eq 12 and the above conditions yields $F_t = 0.38$ and $t = 0.55$ s at the minimum fluorescence, as seen in line 2 of Figure 9. Like the simulation, the analysis yields results contrary to the experimental data.

Simulations of the association reaction (not shown) in accordance with Scheme 6 in which $F'_1 = 1$ (for TA-cal) and $F'_3 = 2.3$ (for TA-cal·P*) gave, as expected, no intermediate fluorescence peak such as that seen in Figure 2B. Thus on both qualitative and quantitative grounds Schemes 5 and 6 are untenable.

Scheme 7

$$\text{TA-cal·P} \underset{k'_{-1}}{\overset{k'_{+1}}{\rightleftharpoons}} \text{TA-cal} + \text{P} \underset{k'_{-2}}{\overset{k'_{+2}}{\rightleftharpoons}} \text{TA-cal·P*}$$

However, there is an alternative mechanism, Scheme 7, which is compatible with the data. In Scheme 7, P binds to TA-cal in two distinct modes that do not interconvert directly. On mixing P with TA-cal the initial phase leads to predominantly TA-cal·P formation, and the observed concentration independent step (controlled by k^*_{obs}, Figure 2) represents the isomerization of TA-cal·P to TA-cal·P* in a flux through TA-cal. The calmodulin trapping experiment (Figure 3B) can be visualized as two independent exponential decays of TA-cal·P and TA-cal·P* in which $k'_{+1} = \lambda_1$ and $k'_{-2} = \lambda_2$. This mechanism was described in theoretical terms by Viale (1971) and discussed in the context of the myosin subfragment 1 ATPase by Bagshaw et al. (1974). As Bagshaw et al. (1974) pointed out, in experiments where fluorescence is monitored, it is difficult to show the predicted concentration dependence of TA-cal·P* formation. Furthermore, as noted above, saturation kinetics are observed in this mechanism just as in Scheme 1. It is therefore difficult to eliminate Scheme 7 as an alternative to Scheme 1. A set of rate constants compatible with data of Figures 2 and 3 is as follows: $k'_{+1} = 6.16\ s^{-1}$, $k'_{-1} = 8.8 \times 10^8\ M^{-1}\ s^{-1}$, $k'_{+2} = 6.2 \times 10^7\ M^{-1}\ s^{-1}$, and $k'_{-2} = 0.61\ s^{-1}$. Also, $F_a = 2.89$, $F_b = 1$, and $F_c = 1.47$ (the relative fluorescence intensities of TA-cal·P, TA-cal, and TA-cal·P*, respectively). These values lead to $F_r = 5.6$ by use of eq 13. Note that the isomerization rate is $(k'_{+1}k'_{+2} + k'_{-2})/(k'_{-1} + k'_{+2}) = 0.98\ s^{-1}$. Whether Scheme 7 is a biologically and physically reasonable alternative to Scheme 1 is not clear; one could, for example, imagine Tyr peptide binding initially with a "wrong" polarity and then reversing itself so that the N-terminus of the peptide interacted with the C-terminal domain of TA-calmodulin. This speculation is, however, somewhat in conflict with the apparent high affinity associated with the initial bimolecular step.

Finally in this discussion about mechanisms we return to an issue raised in analyzing the data of Figure 2. Equation 2 was used to evaluate $(k_{+2} + k_{-2})$, but under conditions where $k_{+1}[P] \approx k_{-1}$, eq 2 is incorrect. For this reason, only data above 65 nM Tyr peptide were used to determine $(k_{+2} + k_{-2})$. Provided that [P] $\gg$ [TA-calmodulin], the correct equations (Halford, 1971) are

for Scheme 1

$$k^*_{obs} = k_{+1}k_{+2}[P]/(k_{+1}[P] + k_{-1}) + k_{-2} \qquad (16)$$

and

for Scheme 5

$$k^*_{obs} = k'_{-1}k'_{-2}/(k'_{+2}[P] + k'_{-2}) + k'_{+1} \qquad (17)$$

In eq 16 k^*_{obs} increases with increasing [P] toward $(k_{+2} + k_{-2})$, while in eq 17 k^*_{obs} decreases with increasing [P] toward k'_{+1} (i.e., k^*_{obs} increases or decreases with increasing [Tyr peptide] depending on the mechanism). The data of Figure 2 favor Scheme 1 in that $k^*_{obs} < 0.99\ s^{-1}$ at lower [Tyr peptide] (e.g., $k^*_{obs} = 0.86\ s^{-1}$ at 20 nM Tyr peptide). Note also that when Scheme 5 is simulated as in Figure 9, eq 17 indicates it would have been preferable to use $k'_{+1} = 1\ s^{-1}$ rather than $k'_{+1} = 0.65\ s^{-1}$. However, the subsequent correction (with $k'_{-1} = 0.58\ s^{-1}$ to keep k'_{+1}/k'_{-1} constant) is minimal with F_r changing from –2.22 to –2.14.

Equilibrium Dissociation Constants of TA-Calmodulin and Calmodulin with Target Peptides and MLCK. Measurement of an equilibrium dissociation constant from the ratios of the dissociation and association rate constants is one of the most reliable methods, especially when the concentrations of interacting species are greater than K_d. The approach we used does not depend on the correct interpretation and identification of the isomerization. It follows that, even if the first-order step seen in Figure 6 were an artifact, the K_d of 0.25–0.56 nM for the TA-calmodulin–MLCK interaction would remain valid. It is noteworthy that within experimental error the K_d value determined by equilibrium measurements of the interaction between TA-calmodulin and Tyr peptide (Figure 1), the one case where that was possible, agreed with the K_d value deduced from the kinetics. The apparent

dissociation constant (k_{-1}/k_{+1}, Scheme 1) of TA-calmodulin and its targets associated with the bimolecular step is within an order of magnitude of the overall K_d. This suggests that most of the interactions between calmodulin and target peptides seen in the atomic resolution structures are probably made in the first step.

The K_m value for calmodulin activating the MLCK-catalyzed phosphorylation of myosin light chains was 3.5 nM and the K_i value for TA-calmodulin as an inhibitor was 12.6 nM. These compare with K_d values of 0.10–0.22 nM and 0.23–0.51 nM for the calmodulin and TA-calmodulin interactions with MLCK and with relative K_d values of 0.43. Conditions of ionic strength, pH, and temperature were essentially the same in the two sets of experiments. Thus there is a positive correlation between the relative (apparent) affinities of calmodulin and TA-calmodulin for MLCK. The K_m for calmodulin is about 20-fold greater than the K_d. The difference between the K_m and K_d values presumably arises because the latter relates to calmodulin binding to free MLCK while for the former MLCK is present as its steady-state complex with myosin light chain and/or nucleotide bound. The difference between the K_i and K_d values for TA-calmodulin is probably for similar reasons in that K_i measurements are made in the presence of MLCK substrates.

Through all the data there is a consistent pattern that calmodulin and TA-calmodulin bind to targets with comparable affinities. Besides the data from Table 1 and from MLCK in the presence of substrates, the K_m values for calmodulin and TA-calmodulin with respect to cyclic AMP phosphodiesterase activity are 0.13 and 0.45 nM respectively. The K_d (or K_m or K_i) values of calmodulin with targets are between 0.28 and 0.88 those of TA-calmodulin. Once K_d values for TA-calmodulin and targets have been measured kinetically, as appears generally feasible, competition experiments between calmodulin and TA-calmodulin lead to reliable K_d values for calmodulin. This is a useful property of TA-calmodulin.

Peptides analogous to Trp peptide have been used to inhibit cellular functions (Itoh et al., 1989; Kargacin et al., 1990; Lorca et al., 1991; McCarron et al., 1992). These peptides each contain the Trp peptide sequence plus a further three to seven amino acids. The Trp peptide is the only one with both its N- and C-terminal amino acids derivatized as amides. The Trp peptide may be more effective than its larger analogues as an inhibitor of cellular function in view of the very high affinity of Trp peptide for calmodulin [cf. the K_d value of 0.006 (±0.002) nM (Table 1) with that of 1.6 (±0.3) nM for peptide RS20 (Lukas et al., 1986)].

Finally, the much greater affinity of Trp peptide compared to Tyr peptide for calmodulin reinforces the key role of the Trp residue in MLCK illustrated, for example, by the inactivity of the W800A mutant of MLCK (Bagchi et al., 1992).

Diffusion-Controlled Association of TA-Calmodulin with Its Target Peptides and MLCK. The second-order rate constant, k_{+1}, for the association of TA-calmodulin and either Tyr peptide or Trp peptide appears to be limited by diffusion (Eigen & Hammes, 1963; Hiromi, 1979). This point could be established more rigorously by analyzing k_{+1} as a function of temperature or viscosity (Dunford & Hewson, 1977; Gutfreund, 1972; Hewson & Dunford, 1975). Where faster associations have been observed, explanations have been sought to explain the phenomenon. For example, in the case of acetylcholinesterase, a combination of aromaticity and positive charge of the ligand were considered important to explain rate constants as high as 2.2×10^9 M^{-1} s^{-1} (Ripoll et al., 1993; Rosenberry & Neumann, 1977; Sussman et al., 1991). The reaction of TA-calmodulin and MLCK also appears to be close to diffusion-controlled and fast compared to typical protein–protein associations (Koren & Hammes, 1976). The rate is 3.6-fold faster than between another modified calmodulin from wheat germ and MLCK (Kasturi et al., 1993) and suggests that fluorescent probes may influence the association kinetics to a minor extent.

We now consider what properties of TA-calmodulin and the target peptides and MLCK may influence the association kinetics. The open conformation of calmodulin (Babu et al., 1988) that closes around the target in the case of MLCK-derived peptides suggests that the recognition occurs more readily than in typical enzyme–substrate complex formation where the need for highly specific binding may be paramount. While the M13 peptide from skeletal muscle myosin light-chain kinase has the propensity to take α-helical structure (Blumenthal et al., 1985), a 17-residue peptide from the N-terminus of the M13 peptide has less than 5% α-helical content in aqueous solution that can be increased to 70% in trifluoroethanol (Klevit et al., 1985; S. R. Martin, personal communication). This suggests that, for the rapid association to occur, the peptide must take a helical conformation during the binding process rather than bind at any one instant only that small fraction of the peptide existing in α-helical form in solution (Burgen et al., 1975).

The structures determined by Ikura et al. (1992) and Meador et al. (1992, 1993) have indicated the importance of ionic interactions. The fact that the association rate as a function of [KCl] passes through a peak suggests that at least two properties play a role (Figure 8). At higher [KCl] it is possible that the favorable interaction of positively charged target peptide with the negatively charged TA-calmodulin binding site will tend to be suppressed, leading to a decrease in the association rate. At lower [KCl] it may be that TA-calmodulin and/or Trp peptide take up a greater proportion of conformations that do not favor diffusion-controlled recognition and complex formation. Hence the observed second-order association rate constant will decrease with decreasing [KCl]. For example, there may be an even higher proportion of random coil to helical substrates among the multiple conformations of Trp peptide (Dyson & Wright, 1991).

To summarize, the associations (Figures 2, 4, and 6) are readily monitored and appear to be diffusion-controlled. As such they provide a useful model to study factors influencing diffusion between calmodulin and its targets.

Thermodynamic, Structural, and Functional Implications of the Isomerization. Stopped-flow studies in which calmodulin and fluorescently labeled plant calmodulins were mixed with skeletal muscle myosin light-chain kinase have characterized the bimolecular association step with rate constants in the range $(1.7–4.6) \times 10^7$ M^{-1} s^{-1} and an isomerization in the range 2.2–7 s^{-1} (Bowman et al., 1992; Johnson et al., 1981). In the case of MLCK only the bimolecular step was observed (Kasturi et al., 1993). The results reported here characterize the mechanism in detail for the reaction of TA-calmodulin and Tyr peptide and by inference indicate that whenever the isomerization is observed, it probably occurs by the mechanism of Scheme 1.

As noted above, from an energetic viewpoint the isomerization is only partially responsible for the higher affinity of TA-calmodulin for Trp peptide compared to its affinity for Tyr-peptide and for MLCK (Table 1). k_{-1}/k_{+1} is at least 50-fold greater for the Tyr peptide than for Trp peptide, while

k_{-2}/k_{+2} is at most 20-fold greater. Comparing the data between MLCK and Trp peptide, k_{-1}/k_{+1} is 45–450-fold greater for MLCK, while k_{-2}/k_{+2} for MLCK equals or is less than that for Trp peptide. At least for TA-calmodulin, the critical role of tryptophan in the target molecule appears to be manifested in the TA-cal·P complex (Scheme 1).

Only limited structural information can be derived from our results. We need to establish whether or not calmodulin·target complexes undergo similar isomerizations to TA-calmodulin·targets before undertaking detailed structure analysis. However, besides the evidence for an isomerization derived from the skeletal muscle myosin light-chain kinase–calmodulin interaction, the comparable K_d (and K_i or K_m) values between calmodulin and TA-calmodulin are circumstantial evidence for an isomerization of calmodulin·MLCK. Kinetic studies with labeled calmodulins in which probes report distances through fluoresence resonance energy transfer (O'Hara et al., 1994) should define to what extent, if any, an isomerization analogous to that described here is responsible for calmodulin being transformed from its open to closed form on binding to MLCK and MLCK-derived peptides.

We now consider whether the isomerization has kinetic significance in smooth muscle physiology. The onset of contraction in smooth muscle has a complex kinetic profile. Activation involving pharmacomechanical coupling (Somlyo & Somlyo, 1968) is characterized by a lag phase of 1–2 s duration at 20 °C followed by a steady, approximately exponential tension development (Somlyo & Somlyo, 1990). Comparison of hormonal activation with activation initiated by rapid photochemical release of D-*myo*-inositol 1,4,5-trisphosphate showed that the major part of the lag phase was determined by events prior to Ca^{2+} release from intracellular Ca^{2+} channels (Somlyo, A. P., et al., 1988). However there was still a lag phase in tension development, albeit of only 200–400 ms, following inositol trisphosphate release.

Kamm and Stull (1986) showed that phosphorylation of myosin light chains is important in determining the rate of tension development. Rate limitation caused by light-chain phosphorylation or an immediately preceding step such as isomerization of a complex of calmodulin·MLCK with its bound substrates has been further substantiated in laser flash photolysis studies. Thus rapid release of ATP into a permeabilized muscle strip, in which MLCK was already activated by calmodulin, induced tension development with a time course similar to that following rapid release of inositol trisphosphate (Somlyo, A. P., et al., 1988; Somlyo, A. V., et al., 1988). The time courses during tension development (i.e., after any lag phase) were similar to those induced pharmacomechanically or by electrical stimulation. On the other hand, tension development was much faster when ATP was released into a muscle strip in which the light chain had been previously thiophosphorylated (Somlyo, A. V., et al., 1988).

It may be that an isomerization of the calmodulin·MLCK complex is responsible for the 200–400-ms lag, which must be caused by an event after the rapid Ca^{2+} release (Somlyo et al., 1992) and rapid Ca^{2+} binding to calmodulin (Johnson et al., 1981; Malencik et al., 1981; Tsurata & Sano, 1990) and before light-chain phosphorylation. The time scale of the lag matches that of the isomerizations recorded here with TA-calmodulin. Whether the isomerization is physiologically relevant depends first on establishing the kinetics of the isomerization at physiological as opposed to 100 μM concentration of Ca^{+} (Somlyo & Himpens, 1989), on identifying the isomerization with calmodulin·MLCK and then showing it occurs in muscle where MLCK may well be associated with other proteins and possibly attached to the myofilament lattice, and finally testing whether the isomerization affects the rate of tension development. Bowman et al. (1992) have provided evidence that phosphorylation of myosin light-chain peptides catalyzed by skeletal muscle myosin light-chain kinase is not limited by a calmodulin-induced isomerization of the kinase. We regard the issue as still unresolved in smooth muscle.

It is also important to know whether the isomerization, if present, has a role in controlling smooth muscle relaxation. It seems clear that Ca^{2+} sequestration from a Ca^{2+}-calmodulin·MLCK complex occurs prior to dissociation of Ca^{2+}-calmodulin from MLCK (Kasturi et al., 1993). Characterization of individual steps, including possible involvement of protein isomerization coupled to Ca^{2+} dissociation, remains to be tackled.

ACKNOWLEDGMENT

We thank Dr. John E. T. Corrie, Dr. Zenon Grabarek, Dr. Andrew Lane, and Dr. Stephen R. Martin for helpful discussions and Mr. Neil A. Trentham for advice in formulating the general theory on relative amplitudes in two-step mechanisms.

REFERENCES

Babu, Y. S., Bugg, C. E., & Cook, W. J. (1988) *J. Mol. Biol. 204*, 191–204.

Bagchi, I. C., Huang, Q., & Means, A. R. (1992) *J. Biol. Chem. 267*, 3024–3029.

Bagshaw, C. R., Eccleston, J. F., Eckstein, F., Goody, R. S., Gutfreund, H., & Trentham, D. R. (1974) *Biochem. J. 141*, 351–364.

Bevington, P. R. (1969) in *Data Reduction and Error Analysis for the Physical Sciences*, McGraw, New York.

Blumenthal, D. K., Takio, K., Edelman, A. M., Chabonneau, H., Titani, K., Walsh, K. A., & Krebs, E. G. (1985) *Proc. Natl. Acad. Sci. U.S.A. 82*, 3187–3191.

Bowman, B. F., Peterson, J. A., & Stull, J. T. (1992) *J. Biol. Chem. 267*, 5346–5354.

Burgen, A. S. V., Roberts, G. C. K., & Feeney, J. (1975) *Nature 253*, 753–755.

Cowley, D. J., & Pasha, I. (1981) *J. Chem. Soc., Perkin Trans. 2*, 918–923.

Cowley, D. J., O'Kane, E., & Todd, R. S. J. (1991) *J. Chem. Soc., Perkin Trans. 2*, 1495–1500.

Dunford, H. B., & Hewson, W. D. (1977) *Biochemistry 16*, 2949–2957.

Dyson, H. J., & Wright, P. E. (1991) *Annu. Rev. Biophys. Biophys. Chem. 20*, 519–538.

Eigen, M., & Hammes, G. G. (1963) *Methods Enzymol. 25*, 1–38.

Fersht, A. R. (1984) in *Enzyme Structure and Mechanism*, 2nd Ed., pp 139–141, Freeman, New York.

Fersht, A. R., & Requena, Y. (1971) *J. Mol. Biol. 60*, 279–290.

Frost, A. A., & Pearson, R. G. (1961) in *Kinetics and Mechanism*, 2nd Ed., pp 173–177, Wiley, London.

Giedroc, D. P., Sinha, S. K., Brew, K., & Puett, D. (1985) *J. Biol. Chem. 260*, 13406–13413.

Giedroc, D. P., Puett, D., Sinha, S. K., & Brew, K. (1987) *Arch. Biochem. Biophys. 252*, 136–144.

Golesworthy, R. C., Shaw, R. A., & Smith, B. C. (1962) *J. Chem. Soc.*, 1507–1508.

Gutfreund, H. (1972) in *Enzymes: Physical Principles*, pp 157–159 and 213–218, Wiley, London.

Halford, S. E. (1971) *Biochem. J. 125*, 319–327.

Halford, S. E. (1972) *Biochem. J. 126*, 727–738.

Hathaway, D. R., & Haeberle, J. R. (1983) *Anal. Biochem. 135*, 37–43.

Hewson, W. D., & Dunford, H. B. (1975) *Can. J. Chem. 53*, 1928–1932.
Hiromi, K. (1979) In *Kinetics of fast enzyme reactions*, pp 261–280, Kodanska, Tokyo.
Ikebe, M., Stepinska, M., Kemp, B. E., Means, A. R., & Hartshorne, D. J. (1987) *J. Biol. Chem. 262*, 13828–13834.
Ikura, M., Clore, G. M., Gronenborn, A. M., Zhu, G., Klee, C. B., & Bax, A. (1992) *Science 256*, 632–638.
Itoh, T., Ikebe, M., Kargacin, G. J., Hartshorne, D. J., Kemp, B. E., & Fay, F. S. (1989) *Nature 338*, 164–167.
Johnson, J. D., Holroyde, M. J., Crouch, T. H., Solaro, R. J., & Potter, J. D. (1981) *J. Biol. Chem. 256*, 12194–12198.
Kamm, K. E., & Stull, J. T. (1986) *Science 232*, 80–82.
Kargacin, G. J., & Ikebe, M., & Fay, F. S. (1990) *Am. J. Physiol. 259*, C315–C324.
Kasturi, R., Vasulka, C., & Johnson, J. D. (1993) *J. Biol. Chem. 268*, 7958–7964.
Kirschner, K., Eigen, M., Bittman, R., & Voight, B. (1966) *Proc. Natl. Acad. Sci. U.S.A. 56*, 1661–1667.
Klee, C. B. (1977) *Biochemistry 16*, 1017–1024.
Klee, C. B. (1988) in *Calmodulin* (Cohen, P., & Klee, C. B., Eds.) Molecular Aspects of Cellular Regulation, Vol. 5, pp 35–56, Elsevier, New York.
Klevit, R. E., Blumenthal, D. K., Wemmer, D. E. & Krebs, E. G. (1985) *Biochemistry 24*, 8152–8157.
Koren, R., & Hammes, G. (1976) *Biochemistry 15*, 1165–1171.
Lorca, T., Galas, S., Fesquet, D., Devault, A., Cavadore, J.-C., & Dorée, M. (1991) *EMBO J. 10*, 2087–2093.
Lowry, T. M., & John, W. T. (1910) *J. Chem. Soc. 97*, 2634–2645.
Lukas, T. J., Burgess, W. H., Prendergast, F. G., Lau, W., & Watterson, D. M. (1986) *Biochemistry 25*, 1458–1464.
Malencik, D. A., Anderson, S. R., Shalitin, Y., & Schimerlik, M. I. (1981) *Biochem. Biophys. Res. Commun. 101*, 390–395.
Mann, D., & Vanaman, T. C. (1987) *Methods Enzymol. 139*, 417–433.
Mann, D., & Vanaman, T. C. (1988) *J. Biol. Chem. 263*, 11284–11290.
Maune, J. F., Klee, C. B., & Beckingham, K. (1992) *J. Biol. Chem. 267*, 5286–5295.
McCarron, J. G., McGeown, J. G., Reardon, S., Ikebe, M., Fay, F. S., & Walsh, J. V. (1992) *Nature 357*, 74–77.
Meador, W. E., Means, A. R., & Quiocho, F. A. (1992) *Science 257*, 1251–1255.
Meador, W. E., Means, A. R. & Quiocho, F. A. (1993) *Science 262*, 1718–1721.
Milos, M., Schaer, J.-J., Comete, M., & Cox, J. A. (1988) *J. Biol. Chem. 263*, 9218–9222.
Newton, D. L., & Klee, C. B. (1989) *Biochemistry 28*, 3750–3757.
O'Hara, P. B., Grabarek, Z., Mabuchi, Y., Macek, V. J., Pianka, G. A., & Hallert, G. E. (1994) *Biophys. J. 66*, A58.
Ripoll, D. R., Faerman, C. H., Axelsen, P. H., Silman, I., & Sussman, J. L. (1993) *Proc. Natl. Acad. Sci. U.S.A. 90*, 5128–5132.
Rosenberry, T. L., & Neumann, E. (1977) *Biochemistry 16*, 3870–3878.
Shaw, R. A., & Ward, P. (1967) *J. Chem. Soc. (B)* 123–126.
Somlyo, A. P., & Somlyo, A. V. (1968) *Pharmacol. Rev. 20* 197–272.
Somlyo, A. P., & Himpens, B. (1989) *FASEB J. 3*, 2266–2276.
Somlyo, A. P., & Somlyo, A. V. (1990) *Annu. Rev. Physiol. 52*, 857–874.
Somlyo, A. P., Walker, J. W., Goldman, Y. E., Trentham, D. R., Kobayashi, S., Kitazawa, T., & Somlyo, A. V. (1988) *Philos. Trans. R. Soc. London, B 320*, 399–414.
Somlyo, A. V., Goldman, Y. E., Fujimori, T., Bond, M., Trentham, D. R., & Somlyo, A. P. (1988) *J. Gen. Physiol. 91*, 165–192.
Somlyo, A. V., Horiuti, K., Trentham, D. R., Kitazawa, T., & Somlyo, A. P. (1992) *J. Biol. Chem. 267*, 22316–22322.
Sussman, J. L., Harel, M., Frolow, F., Oefner, C., Goldman, A., Toker, L., & Silman, I. (1991) *Science 253*, 872–879.
Török, K., Lane, A. N., Martin, S. R., Janot, J.-M., & Bayley, P. M. (1992) *Biochemistry 31*, 3452–3462.
Tsurata, H., & Sano, T. (1990) *Biophys. Chem. 35*, 75–84.
Viale, R. O. (1971) *J. Theor. Biol. 31*, 501–507.
Walsh, M. P., Hinkins, S., Flink, I. L, & Hartshorne, D. J. (1982) *Biochemistry 21*, 6890–6896.
Watterson, D. M., Sharief, F., & Vanaman, T. C. (1980) *J. Biol. Chem. 255*, 962–975.